

Elemental Analysis in Medicinal Materials: Recent Progress and Perspectives

Xiaofang Yang,^{a,#} Xin Liu,^{b,#} Jiayi Hu,^b Fuyao Shi,^a Shengchun Yang,^{b,*} and Xiaodong Wen^{b,*}

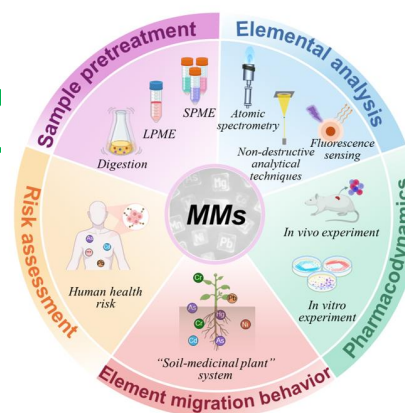
^aDepartment of Histology and Embryology, Dali University, Dali 671000, P. R. China

^bCollege of Pharmacy, Dali University, Dali, Dali 671000, P. R. China

Received: March 24, 2026; Revised: May 12, 2026; Accepted: May 19, 2026; Available online: May 19, 2026.

DOI: 10.46770/AS.2026.0009

ABSTRACT: The elemental composition of medicinal materials (MMs) is directly linked to their therapeutic efficacy and clinical safety, making the development of accurate, efficient, and green analytical strategies of elements critically important. This review systematically evaluates recent methodological advancements in elemental analysis (covering both essential elements and toxic heavy metals) in MMs. Firstly, it highlights innovations in green sample pretreatment technologies, including efficient digestion or extraction techniques. Secondly, it comprehensively compares the performance and application scenarios of various analytical techniques, each offering distinct advantages in sensitivity, multi-element analysis capability, and on-site applicability. Subsequently, the review examined the potential influence of elements on the pharmacological activity of MMs and the migration patterns of various elements in the “soil-medicinal plant” system. Finally, it systematically elaborates on precise health risk assessment models, emphasizing the necessity of shifting from total content analysis to a risk-oriented evaluation paradigm. This review aims to provide a comprehensive reference for the development of green analytical methods, risk assessment, as well as quality and safety control of MMs.



INTRODUCTION

Medicinal materials (MMs) constitute a complex system encompassing herbal (plant-based), animal-derived, and mineral drugs, serving as a vital resource for both global traditional medicine and modern drug discovery. Their clinical efficacy is attributed not only to organic bioactive compounds but is also intrinsically linked to their elemental composition.¹ This composition includes both potentially beneficial essential elements (*e.g.*, Fe, Zn, Cu) and HM elements with well-established human toxicity (*e.g.*, Pb, Cd, As, Hg). These toxic HMs can enter the environment through industrial emissions, agrochemical application, and background soil contamination, subsequently accumulating in medicinal plants and ultimately posing threats to human health *via* the medication chain, causing neurotoxicity, nephrotoxicity, and even carcinogenic effects.^{2,3} Animal-derived medicines may accumulate HMs through

biomagnification in the food chain. Mineral drugs (*e.g.*, cinnabar, realgar) inherently contain HMs in specific chemical forms, where their safety is directly governed by the element's chemical speciation and solubility/release characteristics.⁴ Regardless of their source, excessive levels of toxic elements in MMs can threaten human health upon consumption. Consequently, performing accurate and comprehensive elemental analysis on MMs constitutes the foundation for evaluating their nutritional value and pharmacodynamic potential and simultaneously serves as an essential prerequisite for guaranteeing medication safety and formulating scientific regulatory standards.

However, the complexity and diversity of MM matrices pose multidimensional challenges for elemental analysis. Firstly, regarding sample pretreatment, the intricate organic matrices in plant and animal tissues (*e.g.*, cellulose, proteins) and the stable crystalline structures in mineral drugs demand methods that can

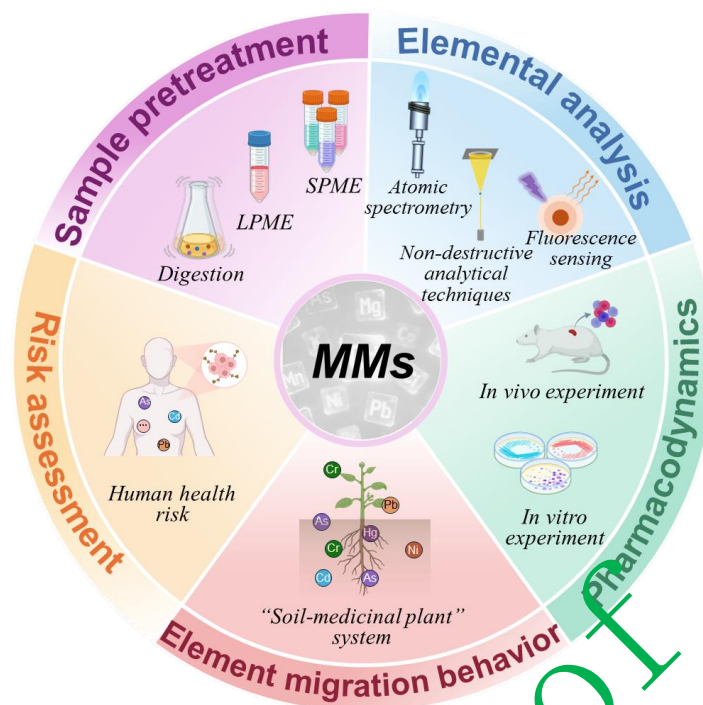


Fig. 1 Schematic diagram of recent advances in elemental analysis of MMs.

completely release target elements while effectively preserving volatile species. Secondly, at the detection level, the trace levels of target elements, coupled with the fact that their chemical speciation dictates bioactivity and toxicity, requires analytical methods to possess high sensitivity, a broad dynamic range, and excellent speciation resolution. Finally, application needs vary from precise laboratory quantification to on-site rapid screening, placing different demands on the efficiency, cost, and portability of the analytical workflow. To address these challenges, traditional approaches combining strong acid digestion with established detection techniques like AAS and ICP-OES remain the cornerstone for total elemental analysis in laboratories.^{5,6} Nevertheless, this paradigm has notable limitations: digestion is often time-consuming, requires large amounts of corrosive reagents, struggles to provide speciation information, and the overall workflow is complex and ill-suited for rapid field analysis.

Currently, the field of analytical chemistry is undergoing a profound evolution towards greening^{7,8} and intelligence⁹ offering novel tools to expand and enhance the elemental analysis capabilities for MMs. In sample pretreatment, novel green solvents like DES and their functionalized variants provide new avenues for developing more efficient and environmentally friendly strategies.¹⁰⁻¹² For detection, ICP-MS has become the core technique for trace analysis due to its exceptional sensitivity,¹³ while the coupling of HPLC with ICP-MS enables precise speciation analysis.¹⁴ Concurrently, emerging technologies such as LIBS,¹⁵⁻¹⁷ XRF,¹⁸⁻²⁰ and molecular fluorescence sensing based on

functional materials^{21,22} offer possibilities for in-situ rapid screening and highly selective on-site detection, respectively. These advancements do not seek to wholly replace traditional methods but aim to build upon them, constructing a multi-tiered modern analytical methodology that ranges from laboratory analysis to field screening, thereby more comprehensively safeguarding the quality and safety of MMs.

This review aims to systematically summarize recent advances in the elemental analysis of MMs (Fig. 1). Firstly, it focuses on novel strategies for green and efficient sample pretreatment, including high-efficiency digestion or extraction techniques based on DES and their switchable variants, as well as the development and application of novel microextraction materials. Secondly, it provides a comprehensive comparison and evaluation of various elemental analysis technologies-including atomic spectrometry, nuclear analytical techniques, and molecular fluorescence sensing techniques-discussing their principles, performance characteristics, and applicability in MMs analysis. Furthermore, it examined the potential influence of elements on the pharmacological activity of MMs and the migration patterns of various elements in the “soil-medicinal plant” system. Finally, it elaborates on how to translate precise analytical data into scientific human health risk assessments and provides an outlook on future trends and challenges in this field. Unlike previous reviews that focus on a single technique or a single matrix, this review systematically integrates the entire analytical workflow-from green pretreatment to multi-technology detection-while connecting analytical data to

the pharmacological activity and health risk assessment of MMs. This cross-disciplinary synthesis, bridging analytical chemistry, environmental science, and clinical safety, lays a more solid scientific foundation for ensuring the quality and safe use of MMs.

SAMPLE PRETREATMENT

In the analysis of MMs, the primary key to accurately determining target components (such as essential elements, toxic HMs, or active substances) lies in establishing efficient and reliable sample pretreatment methods (Table 1). The core objective is to fully release, separate, and enrich the analytes from the complex herbal matrix while minimizing matrix interference and preventing analyte loss. Sample pretreatment typically involves key steps such as digestion, extraction, and concentration. The appropriate selection and systematic optimization of these steps directly determine the sensitivity, accuracy, and overall analytical efficiency of subsequent detection.

Digestion. Digestion is primarily used to decompose the organic matrix of a sample, converting contained mineral elements (especially HMs) into soluble ionic forms suitable for determination by spectroscopy or mass spectrometry.^{37,38} Traditional digestion methods (e.g., wet digestion, microwave digestion) typically employ concentrated acids. While these achieve complete digestion, they suffer from drawbacks such as

operational hazards, high reagent consumption, long processing times, potential loss of volatile elements, and generation of harmful waste.^{39,40} To address these challenges, green solvents, particularly DES and their switchable variants (SDES), have been developed as environmentally friendly and efficient alternative digestion media.⁴¹ DES are usually formed by mixing HBA (e.g., a quaternary ammonium salt) and HBD (e.g., a carboxylic acid, polyol) at a specific molar ratio. They offer advantages such as low toxicity, biodegradability, and ease of synthesis and modulation.⁴²⁻⁴⁴ Their digestion capability stems from a strong hydrogen-bond network and proton-donating/accepting ability, which effectively disrupt plant cell walls, dissolve mineral oxides, and chelate metal ions.

For instance, researchers developed a rapid, simple, and eco-friendly DES-based digestion method for processing *Gentiana rigescens* solid samples. Under optimized conditions, the DES digestates were analyzed by ICP-OES, achieving LODs of 0.40–2.50 $\mu\text{g g}^{-1}$ for Ni, Zn, Co, Cr, and Cu, with spiked recoveries ranging from 90.6% to 111.9%. The quantitative results showed high consistency with those from conventional microwave digestion-ICP-OES, validating the method's accuracy and reliability (Fig. 2a).²³ More innovatively, SDES has been designed as a dual functional solvent capable of simultaneously achieving efficient extraction of target active compounds and rapid digestion of the sample matrix (Fig. 2b).²⁴ Taking the analysis of *Amomi fructus* as an example, researchers synthesized an SDES (e.g., a

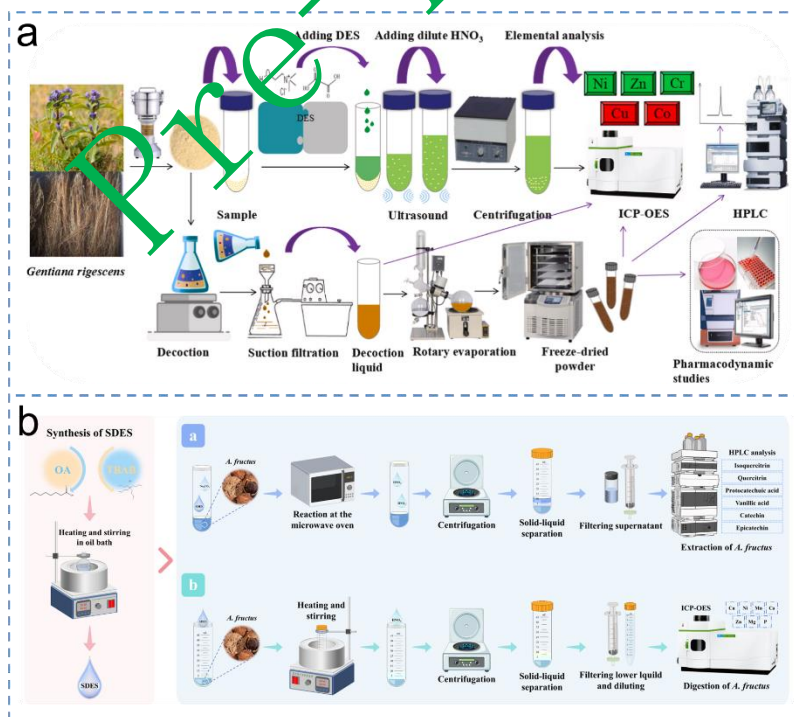


Fig. 2 Schematic diagram of the DES digestion process for (a) *Gentiana rigescens* (adapted with permission from Ref. ²²) and (b) *Amomi fructus* (adapted with permission from Ref. ²³).

Table 1. Comparison of sample pretreatment methods, media, and efficiencies for elemental analysis of MMs

Medicinal materials	Sample pretreatment method	Sample pretreatment media	Analytical technique	Element	Enrichment factor	Recovery	Ref
<i>Gentiana rigescens</i>	DES-based digestion	DES (Choline chloride: oxalic acid = 1:2)	ICP-OES	Ni, Zn, Co, Cr, and Cu	-	90.6%–111.9%	23
<i>Amomi fructus</i>	SDES-based digestion	SDES (Octanoic acid: tetrabutylammonium bromide = 1:3)	ICP-OES	P, Mg, Ca, Mn, Zn, Cu, and Ni	-	-	24
Shirafza, Dineh, and Slim Quick, etc.	LPME	Toluene	GFAAS	Pb, Cr, and Cd	70–500	87%–115%	25
<i>Gastrodia elata</i> Bl.	LPME	DES (Methyltriethylammonium chloride: 1-octanol = 1:2)	Micro UV-vis spectrophotometry	Co	38	92.9%–105%	26
<i>Paris polyphylla</i> var. <i>yunnanensis</i>	LPME	DES (Lidocaine: pelargonic acid = 1:1)	SDIC	Cu	72	90.1%–119.2%	27
<i>Paris polyphylla</i> var. <i>yunnanensis</i> and <i>Salvia yunnanensis</i> C. H. Wright	RS-CPE	DES (L-menthol: nonanoic acid = 2:1)	Micro UV-vis spectrophotometry	Co	38	92.4%–105%	28
<i>Gentiana rigescens</i>	LPME	SHS (Dipropylamine)	Micro UV-vis spectrophotometry	Ni	28	91.6%–110%	29
<i>Salvia miltiorrhiza</i>	LPME	SHS (Nonanoic acid)	Micro UV-vis spectrophotometry	Cu	76.3	94.7%–103.8%	30
<i>Baccharis trimera</i> , <i>Maytenus aquifolia</i> , and <i>Mikania glomerata</i> , etc.	LPME	Cationic ion exchange resin AG50W	FAAS	Pb	2.85	96%–107%	31
<i>Salvia yunnanensis</i> and <i>Amomum villosum</i> Lour.	LPME	SHS (Octanoic acid)	SDIC	Ni	65.1	93.2%–104%	32
<i>Phyllanthus emblica</i> Linn.	MDMSPE	MCOF-DES	ICP-OES	Cu	30	90.6%–106%	33
<i>P. polyphylla</i> var. <i>yunnanensis</i>	DMSPE	GO-TiO ₂ -DES	ICP-OES	Co and Pb	31 and 28	93.9%–105%	34
<i>Polygonatum kingianum</i> Coll. Et Hemsf	MDMSPE	Fe ₃ O ₄ @TiO ₂ @NAD ES	ICP-OES	Pb and Cu	24 and 32	90.3%–107%	35
<i>Ligusticum chuanxiong</i> Hort	DMSPE	Fe ₃ O ₄ @MIL-101(Cr)@PEG	ICP-OES	As, Cd, and Pb	-	-	36

mixture of caprylic acid and tetrabutylammonium bromide). This SDES can be switched to hydrophilic under alkaline conditions (e.g., by adding Na₂CO₃), thoroughly permeating and disrupting plant tissues. Subsequently, under acidic conditions (e.g., by adding HNO₃), it reverts to hydrophobic, enabling efficient extraction of target phenolic compounds for HPLC analysis. Concurrently, the SDES itself serves as a digestion solvent. With mild oil-bath-assisted stirring, complete digestion of the *Amomi fructus* sample can be achieved in merely 5 min, and the digestate can be directly used for ICP-OES determination of various mineral elements (e.g., P, Mg, Ca, Mn, Zn, Cu, Ni). Its digestion efficiency is comparable to microwave digestion but significantly reduces processing time, avoids the use of large amounts of strong acids,

and offers greater safety and environmental friendliness.²⁴

In summary, DES/SDES-based digestion technologies represent an important developmental direction in the pretreatment of MMs samples. They not only address the environmental pollution and operational risks associated with traditional methods but also through flexible coupling with subsequent detection techniques, enable the simultaneous, rapid, and accurate analysis of both active components and risk factors (e.g., HMs) in MMs. This provides robust technical support for establishing a comprehensive quality evaluation system for MMs. Nevertheless, several limitations must be acknowledged. The relatively high viscosity of many DES/SDES systems can hinder

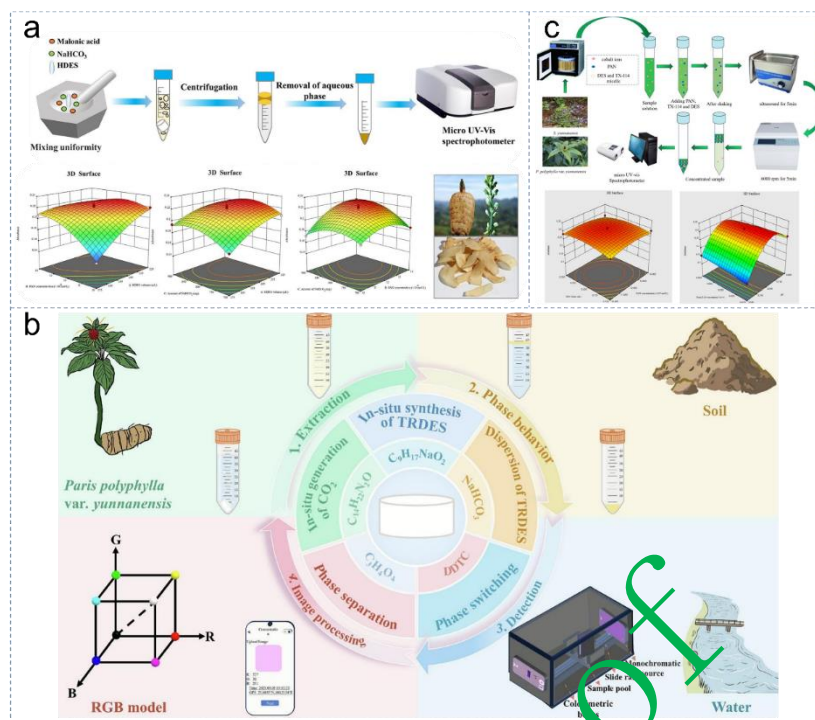


Fig. 3 Schematic of (a) HDES-based effervescent tablet-assisted-LPME procedure for the determination of Co in *Gastrodia elata* Bl. by micro UV-vis spectrophotometry (adapted with permission from Ref.²⁶), (b) effervescent tablet-assisted TRDES-LPME-SDIC for on-site determination of Cu in *Paris polyphylla* var. *yunnanensis* (adapted with permission from Ref.²⁷), and (c) DES-ASSCPE-micro UV-vis spectrophotometry for Co determination in *Paris polyphylla* var. *yunnanensis* and *Salvia yunnanensis* C. H. Wright (adapted with permission from Ref.²⁸).

mass transfer and prolong digestion time, while the potential leaching of DES/SDES components into the sample matrix may introduce analytical interferences. Furthermore, the scalability of DES/SDES-based methods remains underexplored; most studies are conducted at the laboratory scale, and issues such as DES/SDES recyclability, cost-effectiveness, and long-term operational stability have yet to be systematically addressed before these methods can be adopted for routine of industrial applications.

Liquid phase microextraction. To overcome the complexity of MMs matrices and enhance the sensitivity and selectivity of trace element analysis, the application of efficient extraction techniques for the separation and pre-concentration of target analytes following digestion or simple extraction is often necessary.^{45,46} These methods aim to selectively isolate and concentrate target elements from bulk sample solutions, effectively reducing matrix interferences and meeting the requirements of high-sensitivity detection instruments. Current research trends focus on developing novel extraction and enrichment strategies that are green, efficient, automated, or capable of online coupling with detection instruments.

LPME and its derived techniques, which drastically reduce the consumption of organic solvents to microliter levels, enable rapid and efficient enrichment and represent a paradigm of green

analytical chemistry.^{47,48} For example, Aghamohammadi *et al.*²⁵ proposed an ultrasound-assisted emulsification microextraction method. In this approach, trace HMs (e.g., Pb, Cr, Cd) are complexed with a chelating agent, after which a minute amount of extraction solvent (e.g., 45 μ L toluene) is emulsified and dispersed into the aqueous phase *via* ultrasonication. Following centrifugation, only 20 μ L of the organic phase is taken for analysis by GFAAS. This method achieves LOD as low as 0.002–0.03 μ g L⁻¹ for the target metals and enrichment factors up to 70–500, ensuring high sensitivity while significantly reducing the generation of organic waste.²⁵

LPME systems based on green solvents represent another important direction, aiming to replace traditional toxic organic solvents. DES can not only be used for digestion but its hydrophobic variants (HDES) have also been employed as extractants.^{49,50} Notably, switchable DES with environmentally responsive properties (e.g., temperature-responsive TRDES, pH-responsive SDES) further expand their application scope. They can undergo reversible hydrophilic–hydrophobic transitions through external stimuli (e.g., temperature, CO₂), thereby simplifying the recovery of the extraction phase. For example, a HDES with effervescent precursors enabled CO₂-assisted dispersion and extraction of Co from *Gastrodia elata* Bl. (Fig. 3a).²⁶ More innovatively, this concept has been combined with

integrated detection by preparing multifunctional effervescent tablets that incorporate TRDES, effervescent precursors, and chelating agents. Upon addition to the sample solution, these tablets in situ generate CO₂, synthesize TRDES, and form metal complexes. The CO₂ promotes dispersion of the extractant, and phase separation is then achieved through temperature adjustment. The separated organic phase can be directly subjected to quantitative analysis using a modified SDIC device, thereby establishing a complete on-site detection system. This has been successfully applied to the rapid and highly sensitive detection of Cu in environmental water samples, soil, and *Paris polyphylla* var. *yunnanensis* (Fig. 3b).²⁷ Moreover, DES can also serve as a synergistic agent in RS-CPE, working in synergy with the surfactant Triton X-114 at room temperature to rapidly complete the extraction and enrichment of Co from *Paris polyphylla* var. *yunnanensis* and *Salvia yunnanensis* C. H. Wright without the need for heating (Fig. 3c).²⁸

Switchable solvents, particularly SHS, have emerged as a cutting-edge technology in extraction due to their unique environmentally-responsive phase-transition capabilities.^{51,52} SHS (e.g., N,N-dimethylcyclohexylamine, dipropylamine) can reversibly switch between a hydrophilic (ionic) state and a hydrophobic (molecular) state upon triggering by CO₂ or acid-base stimuli. In the hydrophilic state, they mix homogeneously with the sample solution; following triggered phase transition, they instantly form fine droplets of the hydrophobic solvent, efficiently capturing metal complexes. Combined with ultrasound-assisted LPME, this method has been successfully applied for the

determination of trace Ni in MMs (Fig. 4a).²⁹ Integrating SHS precursors into effervescent tablets with smartphone-based colorimetric detection further enabled on-site Cu analysis in *Salvia miltiorrhiza* (Fig. 4b).³⁰ To achieve a higher degree of automation, high throughput, and on-site analysis, various integrated and miniaturized techniques have been developed. The combination of FIA with online pre-concentration technologies has created highly efficient analytical platforms. For instance, the Campos team integrated a cation-exchange resin pre-concentration column into an FIA-FAAS flow path, enabling online enrichment of Pb with a throughput of up to 55 samples per hour.³¹ Demonstrating significant potential for field applications is the integration of SHS effervescent tablet microextraction with SDIC. The color change of the extraction phase is captured by a smartphone, and a custom-developed application establishes a quantitative relationship between concentration and color intensity. This enables rapid, semi-quantitative to quantitative on-site detection of Ni, providing a tool for instant screening at the source of MMs (Fig. 4c).³²

From conventional microextraction to LPME based on green solvents (DES/SHS), and further towards integration with flow injection and smartphone sensing, LPME is rapidly advancing in the direction of greater environmental friendliness, higher efficiency, enhanced intelligence, and improved portability. These technologies have significantly enhanced the selectivity, sensitivity, and operational convenience for analyzing trace elements in the complex matrices of MMs, providing solid and diverse technical support for comprehensive quality and safety control—from laboratory measurement to on-site rapid screening.

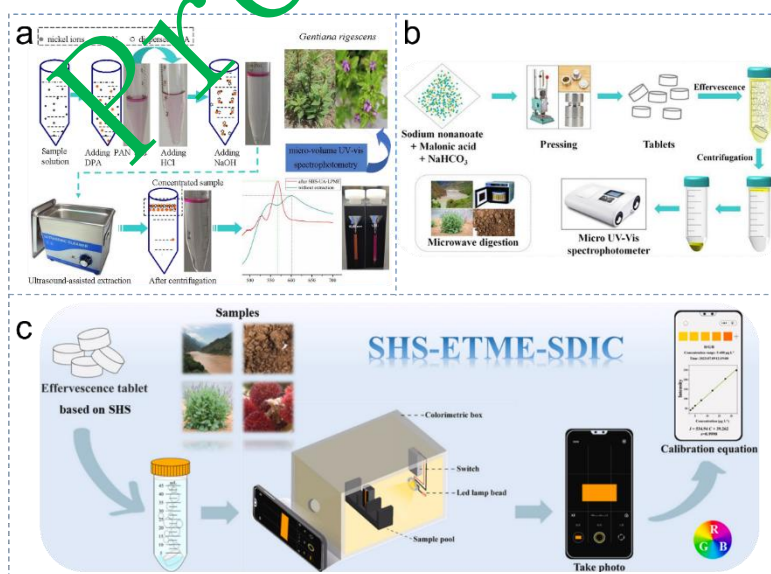


Fig. 4 Schematic of (a) SHS-based LPME-micro UV-vis spectrophotometry for determination of Ni in *Gentiana rigescens* (adapted with permission from Ref. ²⁹), (b) effervescent tablet-assisted-SHS-LPME-micro UV-vis spectrophotometry for determination of Co in *Salvia yunnanensis* (adapted with permission from Ref. ³⁰), and (c) effervescent tablet-assisted-SHS-LPME-SDIC for on-site determination of Ni in *Salvia yunnanensis* and *Amomum villosum* Lour. (adapted with permission from Ref. ³²).

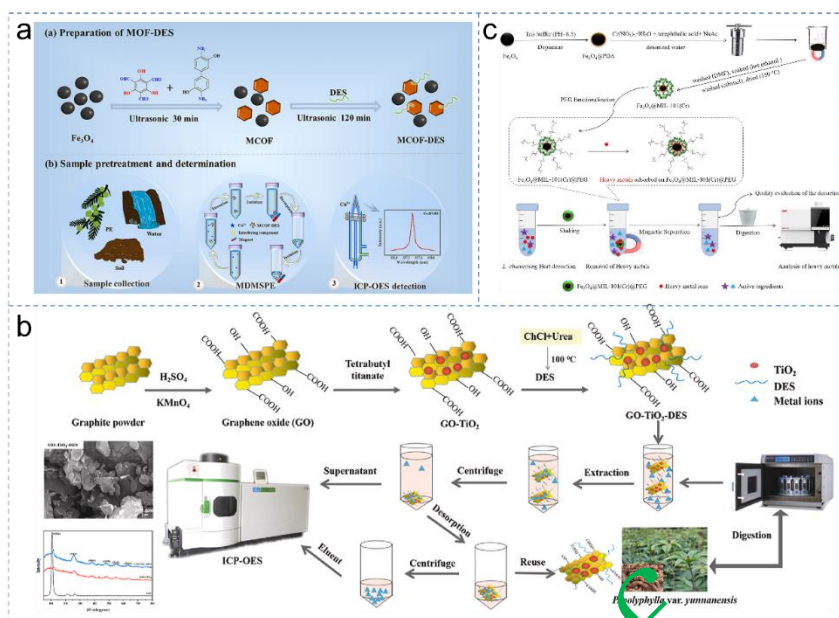


Fig. 5 Schematic of (a) MCOF-DES-based MDMSPE-ICP-OES for determination of Cu in *Phyllanthus emblica* Linn. (adapted with permission from Ref. ³³), (b) GO-TiO₂-DES-based DMSPE-ICP-OES for simultaneous determination of Pb and Co in herbal medicine *Paris polyphylla* var. *yunnanensis* (adapted with permission from Ref. ³⁴), and (c) Fe₃O₄@MIL-101(Cr)@PEG for the efficient removal of As, Cd, and Pb from *Ligusticum chuanxiong* Hort (adapted with permission from Ref. ³⁶).

Dispersive micro-solid phase extraction. DMSPE and its magnetic variant (MDMSPE) have become research hotspots due to their higher mass transfer efficiency and operational convenience.^{102,53} The core of this technology lies in the design and synthesis of high-performance adsorbent materials. Among the strategies, functionalizing adsorbents using DES or NADES is key to enhancing their selectivity and adsorption capacity. DES/NADES can serve as functionalization reagents to modify the surface of various carrier materials, introducing abundant functional groups that enhance affinity toward specific ions.^{54,55} Based on this strategy, various functionalized adsorbents have been successfully developed. A notable example is a novel adsorbent composed of a magnetic covalent organic framework modified with a new DES (MCOF-DES) was first synthesized for the MDMSPE selective enrichment of trace Cu. This material combines the large specific surface area and regular pores of MCOFs with the functionalization sites of DES, exhibiting high selectivity and adsorption capacity for Cu, with an enrichment factor of 30. It enabled accurate determination of Cu in medicinal and edible homologous MMs (*Phyllanthus emblica* Linn.) and environmental samples (soil and water) (Fig. 5a).³³ Similarly, DES was modified onto a GO-TiO₂ nanocomposite to synthesize a novel GO-TiO₂-DES adsorbent for the DMSPE simultaneous enrichment of trace Co and Pb in *P. polyphylla* var. *yunnanensis*, achieving enrichment factors of 31 and 28 for the two elements, respectively (Fig. 5b).³⁴ Furthermore, by modifying a magnetic Fe₃O₄@TiO₂ composite with NADES, the prepared Fe₃O₄@TiO₂@NADES adsorbent exhibited excellent adsorption

performance for Pb and Cu in *Polygonatum kingianum* Coll. Et Hemsl., with enrichment factors of 24 and 32, respectively.³⁵ These studies demonstrate the great potential of custom-designing adsorbents *via* DES/NADES to achieve efficient and selective enrichment of multiple target elements in complex MM matrices. Notably, NADES are more environmentally friendly than DES due to their natural composition, lower toxicity, and biodegradability.

Moreover, SPME technology serves not only analytical detection but its principle can also be directly applied to the selective removal of HM contaminants from herbal decoctions to ensure clinical medication safety. A representative example is the designed and synthesized a polyethylene glycol-functionalized magnetic nanocomposite, Fe₃O₄@MIL-101(Cr)@PEG. This material possesses a porous structure and a large specific surface area, enabling efficient adsorption of As⁵⁺, Cd²⁺, and Pb²⁺ from *Ligusticum chuanxiong* Hort decoction (removal rate >81%), while causing minimal loss of key active constituents (e.g., Senkyunolide and Ferulic acid, <8%). The loss rate of total solids in the decoction was only 0.18%, and the fingerprint similarity remained above 99.9%. This provides a low-cost, simple-operation, novel pathway for selectively removing exogenous HM pollutants without compromising the pharmacologically active substances of MMs (Fig. 5c).³⁶ Taken together, DMSPE/MDMSPE based on novel functionalized adsorbent materials has become an indispensable, highly efficient enrichment tool in the analysis of trace elements in MMs.

Simultaneously, the technology is expanding into more challenging application scenarios, such as the selective removal of harmful HMs from complex MM systems. This reflects its dual application value in the field of MM quality and safety control, spanning from “analytical detection” to “purification treatment”.

ELEMENTAL ANALYSIS

Based on efficient and green sample pretreatment, accurate and sensitive elemental analysis techniques are essential for the quality evaluation and safety risk monitoring of MMs. According to differences in detection principles and application scenarios, the techniques currently employed for elemental analysis of MMs can be broadly classified into three categories: atomic spectrometry/mass spectrometry (including AAS, AFS, ICP-OES, ICP-MS, and LIBS), nuclear analytical techniques (including PIXE-PIGE, XRF, and INAA), and molecular fluorescence sensing techniques (Table 2). Each category possesses distinct advantages in terms of sensitivity, multi-element simultaneous analysis capability, sample consumption, cost, and field applicability. In practice, these techniques often complement one another, collectively forming a multi-tiered analytical system that spans from precise laboratory quantification to rapid on-site screening.

Atomic spectrometry. Atomic spectrometry, owing to its high sensitivity, good selectivity, and relatively straightforward operation, has become the most fundamental tool for elemental analysis in MMs.

Among these techniques, AAS is one of the most long-standing and mature analytical methods, primarily including FAAS and GFAAS. The former is typically used for the determination of essential elements at higher concentrations, while GFAAS, with its superior sensitivity, is specialized for detecting trace-level elements in MMs.⁸¹⁻⁸³ Numerous studies have successfully employed AAS to assess the element (such as HM) contamination status of medicinal plants from different regions. For instance, analysis of medicinal plants grown across Austria *via* AAS showed generally low levels of toxic elements Pb and Cd. In most samples, Cd and Pb contents were below 0.20 mg kg⁻¹ and 1.50 mg kg⁻¹ on a dry weight basis, respectively, although certain species like St. John's wort and poppy exhibited a stronger tendency for Cd accumulation.⁵⁶ Similarly, analysis of elements in different parts of rosemary from Jordan revealed distribution patterns: Pb, Zn, Cu, and Cd were primarily enriched in the flowers and leaves. By correlating soil and plant samples, the study also illuminated the translocation characteristics of these elements.⁵⁷ Furthermore, AAS has been widely used to evaluate the significant impact of different growing environments (*e.g.*, wastewater-irrigated vs. clean water-irrigated areas) on the element content of medicinal plants, highlighting the importance

of environmental control.⁵⁸ Although some studies indicate that the element content in MMs from specific regions may be below the limits set by organizations like the WHO, suggesting a low direct risk to human health, this precisely underscores the necessity for ongoing monitoring using reliable analytical methods such as AAS.^{59,60} In summary, as a mature and reliable analytical approach, AAS continues to play an indispensable role in the screening of element contamination in medicinal plants, research on their translocation patterns, and preliminary safety assessments.

A high-performance detection method for elements such as As that can form volatile hydrides is AFS, particularly when coupled with HG-AFS.^{84,85} Its working principle is based on the reduction of the target element to a gaseous hydride, which is then atomized and excited by a specific light source to generate a fluorescence signal for quantitative analysis. The core advantages of HG-AFS lie in its extremely high sensitivity, excellent selectivity, and strong capability to withstand complex sample matrices.^{86,87} In the analysis of elements in medicinal plants and mineral drugs, this technique has proved to be a crucial tool for studying element bioaccessibility, *in vivo* metabolism, and risk assessment. A case in point is the study investigating the leaching characteristics of traditional MMs and their compound preparations containing cinnabar (HgS) and realgar (As₂S₂/As₄S₄), HG-AFS can accurately determine the trace amounts of As and Hg dissolved in different artificial digestive fluids (gastric, intestinal, and intestinal fluids containing trypsin). Its detection performance is comparable to that of ICP-MS, yet it offers advantages in terms of operational costs.⁶¹ More importantly, HG-AFS demonstrates irreplaceable value *in vivo* pharmacokinetic and risk assessment studies. A study on AnGongNiuHuang Pill, a preparation containing realgar and cinnabar, employed HG-AFS to determine the As and Hg contents in rat blood and urine. It revealed that this compound formulation could significantly reduce the absorption of As and promote its urinary excretion, while simultaneously increasing the absorption of Hg and reducing its urinary excretion. This provides critical pharmacokinetic data for scientifically evaluating the clinical safety of such mineral-containing medicines.⁶² Although its linear dynamic range is generally narrower than that of ICP-MS and it is primarily limited to specific elements, HG-AFS, by virtue of its high cost-effectiveness, low susceptibility to interference, and reliable stability, has become an indispensable key technology for the specialized analysis of As and Hg in MMs, studies on their speciation distribution, and health risk assessments.

With its wide dynamic linear range, capability for simultaneous multi-element analysis, and relatively low operational cost, ICP-OES serves as an ideal tool for determining major and trace elements.^{88,89} A case in point a study on five medicinal plants from Ethiopia utilized ICP-OES to accurately determine the contents of elements such as Fe, Zn, Cu, and Mn in their roots and leaves. Method validation showed good recovery rates, providing reliable

Table 2. Comparison of sample pretreatment methods and media, analytical techniques and their performance, and applicable scenarios for elemental analysis of MMs

Medicinal materials	Sample pretreatment method	Sample pretreatment media	Analytical technique	Element	Limit of detection	Relative standard deviation	Linear correlation coefficients	Recovery	Applicable scenarios	Ref
<i>Carum carvi</i> , <i>Hypericum perforatum</i> , and <i>Mentha piperita</i> , etc.	Microwave digestion	HNO ₃ and H ₂ O ₂	AAS	Cd, Cu, Fe, Mn, Pb, and Zn	-	-	-	-	Routine elemental quantification, laboratory analysis	56
<i>Rosmarinus officinalis labiatae</i>	Acid digestion	HNO ₃ and HCl	AAS	Pb, Cu, Zn, Cd, Ni, and Fe	-	-	> 0.9998	93.3%–97.7%	Routine elemental quantification, laboratory analysis	57
<i>Medicago polymorpha</i> L., <i>Mentha longifolia</i> L., <i>Vicia sativa</i> L., and <i>Oxalis corniculata</i> L.	Acid digestion	HNO ₃ , H ₂ SO ₄ , and HClO ₄	AAS	Mn, K, Na, Zn, Co, Fe, and Cu	-	-	-	-	Routine elemental quantification, laboratory analysis	58
<i>Dichrostachys cinerea</i> , <i>Maerua angolensis</i> , and <i>Mimulus zeyheri</i> , etc.	Acid digestion	HCl and HNO ₃	AAS	Cr, Pb, As, and Ni	-	-	-	-	Routine elemental quantification, laboratory analysis	59
<i>Bacopa monnieri</i> , <i>Hippophae rhamnoides</i> , and <i>Dioscorea bulbifera</i>	Wet digestion	HCl and HNO ₃	AAS	Fe, Cu, Mn, Zn, Ni, Co, Mo, V, Cr, As, Pb, Hg, and Cd	-	-	-	-	Routine elemental quantification, laboratory analysis	60
Realgar and cinnabar	Microwave digestion	Aqua regia and HNO ₃	HG-AFS, ICP-MS	As and Hg	0.002–0.32 µg L ⁻¹	< 5.7%	≥ 0.999	72%–97%	Ultra-trace multi-element analysis, laboratory analysis	61
Realgar, cinnabar, and AnGongNiuHuang Pill	Modified fast Kjeldahl digestion	HNO ₃ and HClO ₄	HG-AFS	As and Hg	0.0019–0.017 µg mL ⁻¹	< 10%	> 0.999	95%–111%	Volatile element analysis, laboratory analysis	62
<i>Asparagus africanus</i> , <i>Ferula communis</i> , and <i>Stephania abyssinia</i> , etc.	Acid digestion	HCl, HNO ₃ , and HClO ₄	ICP-OES	Fe, Zn, Cu, and Mn	0.0003 – 0.072 mg kg ⁻¹	-	≥ 0.98	92%–114.6%	Multi-element analysis, laboratory analysis	63
<i>Glycyrrhiza glabra</i> L. Fabaceae, <i>Laurus nobilis</i> L. Lauraceae, and <i>Rhus coriaria</i> L. Anacardiaceae	Microwave digestion	HNO ₃	ICP-OES	Al, B, Ca, Cd, Cr, Cu, Fe, K, Mg, Mn, Na, Ni, Pb, and Zn	-	-	-	-	Multi-element analysis, laboratory analysis	64
<i>Arbutus unedo</i> L. Ericaceae, <i>Cercis siliquastrum</i> L. Fabaceae, and <i>Cichorium intybus</i> L. Asteraceae	Microwave digestion	HNO ₃	ICP-OES	Al, B, Ca, Cd, Cr, Cu, Fe, K, Mg, Mn, Na, Ni, Pb, and Zn	0.010 – 0.608 mg kg ⁻¹	< 2.24%	> 0.999	-	Multi-element analysis, laboratory analysis	65
Compound Niu Huang Xiaoyan Capsule	Microwave digestion	-	ICP-MS	As and Hg	-	< 5%	> 0.998	95%–105%	Ultra-trace multi-element analysis, laboratory analysis	66

<i>Carissa spinarum</i> L., <i>Myrothamus flabellifolia</i> Welw., and <i>Callilepis laureola</i> DC., etc.	Acid digestion	HNO ₃ , HClO ₄ , and H ₂ O ₂	ICP-MS	Mn, As, Cd, Cu, Pb, Ni, Zn, Hg, and Cr	-	-	-	-	Ultra-trace multi-element analysis, laboratory analysis	67
Mistletoe	Wet digestion	HNO ₃ and H ₂ O ₂	ICP-OES, ICP-MS	Al, As, B, Ba, Ca, Cd, Co, Cr, Cu, Fe, K, Mg, Mn, Mo, Ni, Sr, Pb, Ti, and Zn	-	-	-	-	Ultra-trace multi-element analysis, laboratory analysis	68
<i>Coptidis</i>	Pressed tablet	-	RDP-LIBS	Cu, and Pb	1.91 – 3.03 mg kg ⁻¹	< 7.8%	> 0.9926	-	Suitable for field screening and elemental mapping	69
<i>Angelica sinensis</i> and <i>Scutellaria baicalensis</i>	Pressed tablet	CuSO ₄ ·5H ₂ O	LIBS	Cu	-	< 14.32%	> 0.94	-	Suitable for field screening and elemental mapping	70
<i>Plantago erosa</i> Wall, <i>Emblca officinalis</i> Gaertn, and <i>Ocimum gratissimum</i> , etc.	Pressed pellet	Polyvinyl alcohol	PIXE-PIGE	K, Ca, Mn, Fe, Zn, Cu, Na, Mg, Al, and P	-	< 1.0%	-	-	Non-destructive analysis, suitable for precious samples	71
<i>Croton dioicus</i> and <i>Phoradendron villosum</i>	Pressed pellet	-	XRF	Cu and Ni	1.01 – 0.63 mg kg ⁻¹	-	> 0.996	-	Non-destructive and multi-element analysis, suitable for solid samples and distribution mapping	72
<i>Hemerocallis minor</i> Miller	Pressed pellet	-	XRF	Fe, Ti, Mn, Cr, Cu, Ni, Zn, Sr, and Ba	-	-	-	-	Non-destructive and multi-element analysis, suitable for solid samples and distribution mapping	73
<i>Acanthus ilicifolius</i> , <i>Avicennia officinalis</i> , and <i>Xylocarpus mekongensis</i>	-	-	INAA and AAS	Al, As, Br, Ca, Cd, Ce, Co, Cr, Fe, K, La, Mn, Pb, Sb, Sc, Sm, Th, V, and Zn	-	-	-	-	Non-destructive analysis, routine elemental quantification	74
<i>Niu Huang Jiedu Pian</i> and <i>Liushen wan</i>	-	-	INAA	Cr, Co, As, Sb, and Hg	-	-	-	-	Non-destructive analysis	75
<i>Astragalus</i> and <i>Paeonia lactiflora</i>	Microwave digestion	HNO ₃	Fluorescent sensing	Cu	0.225 μM	< 0.98%	0.9940	93.85%– 106.75%	Suitable for specific ions on-site analysis	76
<i>Fufang-Shuanghua pill</i> and <i>Changyanning pill</i>	-	-	Fluorescent sensing	Hg	2.2 nM	< 9.5%	0.997	99.3%– 107.5%	Suitable for specific ions on-site analysis	77
<i>Paris polyphylla</i> var. <i>yunnanensis</i>	Microwave digestion	HNO ₃ and H ₂ O ₂	Fluorescent sensing	Cu	6.78 μM	< 3.65%	0.9952	92.0%– 109%	Suitable for specific ions on-site analysis	78
<i>Salviae miltiorrhizae Radix et Rhizoma</i>	Microwave digestion	HNO ₃ and H ₂ O ₂	Fluorescent sensing	Co	4.51 μM	< 3.51%	0.998	97.8%– 106%	Suitable for specific ions on-site analysis	79
<i>Panax notoginseng</i>	-	-	Fluorescent sensing	Cd	0.89 μg L ⁻¹	-	0.992	96.5%– 104.09%	Suitable for specific ions on-site analysis	80

Table 3. Effects of elements on the pharmacodynamics of MMs, together with their migration behavior and human health risk assessment.

Medicinal materials	Sample pretreatment	Analytical technique	Element	Other	Ref
<i>Holarrhena pubescens</i> and <i>Wrightia tinctoria</i>	Microwave digestion	ICP-OES	Cr, Cu, Fe, Mn, Ni, Pb, and Zn	Pharmacodynamic evaluation	117
<i>Tussilago farfara</i> L.	Acid digestion	AAS	Cu, Zn, Fe, Mn, Pb, and Cd	Pharmacodynamic evaluation	118
<i>Gentiana rigescens</i>	Microwave digestion	ICP-OES	Pb	Pharmacodynamic evaluation	119
<i>Polygonatum kingianum</i>	Microwave digestion	ICP-OES	Cu, Pb, Fe, Cr, Al, Co, Zn, Mn, Ni, and Cd	Pharmacodynamic evaluation	120
<i>Paris polyphylla</i> var. <i>Yunnanensis</i>	Microwave digestion	ICP-OES	Cu, Al, Cr, Mn, Fe, Co, and Zn	Pharmacodynamic evaluation	121
<i>Coriandrum sativum</i> L.	Acid digestion	AAS	Cd and Pb	Pharmacodynamic evaluation	122
<i>Lavandula dentata</i> L.	Acid digestion	AAS	Zn, Cu, Cd, and Pb	Pharmacodynamic evaluation	123
<i>Paeonia Lactiflora</i> Pall.	Acid digestion	ICP-MS	Al, Fe, Mn, Cu, Pb, Zn, As, and Cd	Element migration behavior study	124
<i>Gastrodia elata</i>	-	ICP-MS, AFS	Cd, Cu, As, Hg, and Pb	Element migration behavior study	125
<i>Epimedium</i>	Acid digestion	ICP-MS	Cr, Ni, Cu, As, Pb, and Zn	Element migration behavior study	126
<i>Houttuynia cordata</i> Thunb.	Microwave digestion	ICP-OES	Zn, Ni, Pb, Cu, Cr, Fe, Mn, and Co	Element migration behavior study	127
<i>Polygonatum cyrtoneura</i> Hua and <i>Bletilla striata</i>	Electric hot plate digestion	ICP-OES	Cd	Element migration behavior study	128
<i>Panax notoginseng</i>	Acid digestion	GF-AAS	Cd	Element migration behavior study	129
<i>Ligusticum sinense</i> cv. <i>Chuanxiong</i>	-	-	Cd	Element migration behavior study	130
<i>Ligusticum sinense</i> cv. <i>Chuanxiong</i>	-	-	Cd	Element migration behavior study	131
Ginseng	Microwave digestion	ICP-MS	Cu, Zn, Ni, Cr, Pb, As, Cd, and Hg	Element migration behavior study	132
<i>Bauhinia forficata</i> , <i>Eleusine Indica</i> , and <i>Orthosiphon stamineus</i>	Microwave digestion	ICP-OES	K, Mg, Na, P, Al, Fe, Zn, Mn, Cu, Ni, and Se	Human health risk assessment	133
<i>Tribulus terrestris</i> , <i>Allium sativum</i> , and <i>Aloe barbadensis</i>	Acid digestion	AAS	Zn, Fe, and Pb	Human health risk assessment	134
<i>Aster tataricus</i> L.f., <i>Salvia miltiorrhiza</i> Bge, and <i>Radix Aucklandiae</i> , etc.	Microwave digestion	ICP-MS	Cr, Ni, Cu, Zn, As, Cd, Hg, and Pb	Human health risk assessment	135
<i>Azadirachta indica</i> , <i>Ocimum viride</i> , and <i>Alchornea cordifolia</i> , etc.	Acid digestion	ICP-MS	Cd, Cr, Hg, Mn, Ni, and Pb	Human health risk assessment	136
<i>Adiantum capillus-veneris</i> L., <i>Alcea apterocarpa</i> (Fenzl) Boiss., and <i>Ammi visnaga</i> (L.) Lam., etc.	Microwave digestion	ICP-OES	Al, B, Ca, Cd, Cr, Cu, Fe, K, Mg, Mn, Na, Ni, Pb, and Zn	Human health risk assessment	137
<i>Panax notoginseng</i>	Acid digestion	AFS	As, Cd, Cu, Hg, Ni, Pb, and Zn	Human health risk assessment	138
<i>Cordyceps sinensis</i>	Microwave digestion	ICP-MS	Cu, Pb, As, Cd, and Hg	Human health risk assessment	139
<i>Pheretima aspergillum</i> , <i>Curcuma kwangsiensis</i> , and <i>Oldenlandia diffusa</i>	Microwave digestion	ICP-MS	Pb, Cd, and As	Human health risk assessment	140

data for assessing the nutritional value and potential metal exposure of these plants.⁶³ Numerous investigations have also confirmed that ICP-OES can effectively reveal the impact of environmental factors on element accumulation in medicinal plants. For example, samples collected near industrial areas, mining regions, or farmlands often exhibit higher concentrations of HMs.^{64,65} In contrast, ICP-MS holds a dominant position in the precise determination of trace and ultra-trace levels of elements and in health risk assessments, due to its extremely high sensitivity, even wider linear range, and capabilities for isotope analysis and elemental speciation.^{90,91} This technique is particularly suitable for critical safety evaluation scenarios that require distinguishing between total element content and bioaccessible fractions. As demonstrated by evaluating the compound preparation Niu Huang Xiaoyan Capsule containing realgar and cinnabar, researchers employed two sample pretreatment methods—microwave digestion and semi-bionic extraction—to prepare samples separately. ICP-MS was then used to accurately determine the total As, total Hg, and the soluble As and Hg contents in artificial gastric fluid. The analysis results indicated that the contents of soluble As and Hg were significantly lower than the total amounts. This provides direct evidence for a scientifically based risk assessment of such mineral-containing medicines using bioaccessibility data, highlighting the value of ICP-MS in addressing complex safety issues related to MMs.⁶⁶ Other applications further demonstrate its powerful functionality. ICP-MS analysis of medicinal plants used in South Africa for treating skin cancer not only accurately quantified the levels of As, Cd, Pb, and Cr but also enabled the calculation of the target THQ based on this data, facilitating a systematic health risk evaluation.⁶⁷ ICP-OES and ICP-MS are also frequently used in combination to leverage their respective strengths. In a study on mistletoe and its host almond tree, ICP-OES was employed to determine major elements, while ICP-MS was used for trace elements like As and Cd, thereby comprehensively evaluating the translocation and enrichment behaviors of elements within the parasitic system.⁶⁸ In brief, ICP-OES and ICP-MS together constitute a powerful and complementary technical system in the current analysis of elements in MMs. They provide essential technical support for quality control, environmental tracing, and safety assessment.

Based on the ablation of a sample by high-energy laser pulses to generate plasma, followed by analysis of its emission spectrum for the qualitative and quantitative determination of elements, LIBS is an atomic spectrometry technique.⁹²⁻⁹⁴ In the field of elemental analysis, LIBS has gained prominence due to its capabilities for rapid, in-situ, minimally destructive or nearly non-destructive analysis, the elimination of complex sample preparation, and simultaneous multi-element detection.^{95,96} The analytical performance can be effectively enhanced by optimizing laser parameters (e.g., energy, pulse interval, detection delay). For instance, the application of RDP-LIBS for detecting Cu and Pb in

Coptidis significantly increased spectral line intensities compared to single-pulse LIBS, achieving lower detection limits of 1.91 mg kg⁻¹ and 3.03 mg kg⁻¹, respectively, thereby meeting the detection requirements of relevant industry standards.⁶⁹ However, LIBS spectra are susceptible to matrix effects and self-absorption effects, posing challenges to quantitative accuracy. Unlike the gold-standard ICP-MS (ultra-high sensitivity, but laboratory-bound and requiring digestion), LIBS prioritizes speed and on-site applicability over ultra-trace precision. Consequently, employing chemometric methods (such as partial least squares regression, artificial neural networks) to establish multivariate calibration models has become a key strategy for improving the reliability of LIBS quantitative analysis. Research has demonstrated that LIBS combined with back-propagation artificial neural networks yields predicted values for Cu in *Angelica sinensis* and *Scutellaria baicalensis* that are closer to the true values, significantly outperforming traditional univariate calibration curve methods.⁷⁰ Therefore, as an emerging “chemical fingerprinting” technique for rapid screening, LIBS demonstrates considerable potential in the geographical differentiation of medicinal plants, rapid on-site early warning of element contamination, and online monitoring. A practical strategy is to use LIBS for field triage followed by laboratory-based ICP-MS for targeted confirmation, balancing speed with accuracy.

Non-destructive analytical techniques. Particle accelerator-based nuclear analysis techniques, particularly PIXE and PIGE, provide a unique non-destructive analytical approach for multi-element analysis of MMs. PIXE, by detecting characteristic X-rays emitted from a sample upon proton excitation, is primarily used for analyzing elements with higher atomic numbers (e.g., transition metals).^{97,98} In contrast, PIGE measures characteristic γ -rays produced from proton-induced nuclear reactions, making it especially sensitive to light elements.^{99,100} These two techniques offer complementary advantages, and their combined use enables coverage of a broader elemental range.^{71,101} Their most significant advantage lies in the extremely simple sample preparation (typically requiring only drying, grinding, and pelletizing), completely avoiding issues associated with conventional wet digestion such as potential contamination, loss, and inaccurate determination of volatile elements. This ensures the authenticity and reliability of the analytical results. For example, PIXE-PIGE analysis of seven medicinal plants from northeastern India successfully determined the contents of various major and trace elements, including K, Ca, Mn, Fe, Zn, Cu, Na, Mg, Al, and P, providing crucial data for assessing their nutritional value and potential pharmacological roles (e.g., iron supplementation, gastric acid neutralization).⁷¹ However, the widespread application of this technology is constrained by its reliance on large-scale accelerator facilities, high equipment and maintenance costs, and relatively low analysis throughput. Therefore, while PIXE-PIGE is not the primary choice for routine testing, it holds irreplaceable

value as a high-precision, non-destructive reference method in fundamental elemental composition surveys of MMs, analysis of precious samples, and methodological comparison studies.

Based on the emission of characteristic X-rays from a material excited by high-energy X-rays, XRF is an analytical method for the qualitative and quantitative determination of elements.¹⁰²⁻¹⁰⁴ In elemental analysis, particularly energy dispersive XRF, it has attracted significant attention due to its notable characteristics of being non-destructive, rapid, capable of simultaneous multi-element determination, and requiring no complex sample digestion.¹⁰⁵ This technique allows for the direct, in-situ, and non-destructive analysis of solid powder pellets or intact plant tissues. It can not only determine the total content of various elements but is also effectively used to study the spatial distribution of elements within different organs of medicinal plants (e.g., root, stem, leaf, flower).^{72,73} A case in point is the application of XRF to analyze the Mexican medicinal plants *Croton dioicus* and *Phoradendron villosum*, enabling a rapid assessment of their Cu, Ni, and other element levels.⁷² Another study utilized XRF to reveal differences in the distribution of various elements like Fe, Mn, Cr, and Cu across different parts of *Hemerocallis minor* Miller, as well as their dynamic changes over sampling time.⁷³ However, the sensitivity of XRF is generally lower than that of atomic spectrometric and mass spectrometric techniques (e.g., ICP-MS), limiting its detection capability for trace elements (especially Cd, Hg, etc.). Furthermore, it is significantly affected by matrix effects, often requiring calibration with certified reference materials for quantitative analysis. Therefore, the advantages of XRF in the element analysis of MMs primarily lie in rapid screening, in situ distribution mapping, non-destructive analysis of precious or minute samples, and preliminary environmental risk assessment. It serves as a valuable complement to existing high-sensitivity, destructive analytical techniques.

Occupying a unique position in elemental analysis, NAA, particularly INAA, is a non-destructive analytical technique based on nuclear reactions.¹⁰⁶⁻¹⁰⁸ Its principle involves irradiating a sample with thermal neutrons and subsequently measuring the characteristic gamma rays emitted by the induced radionuclides to achieve qualitative and quantitative determination of elements. The outstanding advantages of NAA include the elimination of complex chemical digestion, simple sample preparation (typically requiring only drying, grinding, and weighing), effective avoidance of reagent contamination and volatilization losses, as well as exceptionally high sensitivity, accuracy, and excellent multi-element simultaneous analysis capabilities.¹⁰⁹ These characteristics make it particularly suitable for the concurrent determination of a wide range of elements, from major to trace levels (including essential elements and heavy metals), in plant matrices.

For example, INAA and AAS were employed to determine the

contents of essential and toxic elements (including 20 elements such as Al, As, Cr, Fe, Zn) in three medicinal plants (*Acanthus ilicifolius*, *Avicennia officinalis*, and *Xylocarpus mekongensis*). Based on these data, the THQ was calculated to systematically assess the associated health risks.⁷⁴ Another study involving INAA screening of various MMs accurately revealed the abnormal enrichment of key toxic elements such as As and Hg; specifically, the As content in Niuhuang Jiedu Pian was found to be as high as approximately 8.3%.⁷⁵ However, the widespread application of INAA is constrained by inherent limitations: a heavy reliance on nuclear reactor facilities, high equipment and maintenance costs, long analysis turnaround times (depending on nuclide half-lives), and difficulty in analyzing certain specific elements. Consequently, INAA is not the primary choice for routine testing but serves as an authoritative reference method for the certification of reference material values and for validation through data comparison across different analytical techniques (e.g., ICP-MS and AAS). It also plays a critical role in multi-element survey studies and in the arbitration analysis of samples with contentious results. With its characteristics of being virtually free from matrix interference and offering high accuracy, INAA provides a benchmark for establishing a reliable quality control system for the elemental analysis of medicinal plants.

Fluorescence sensing techniques. Fluorescence sensing technologies based on specific optical responses have demonstrated significant advantages in the rapid screening and selective detection of target analytes, owing to their high selectivity, sensitivity, and operational simplicity.^{110,111} Compared with conventional atomic spectrometric methods, such techniques primarily rely on the rational design of molecular or nanoprobe. These probes selectively interact with target elements (e.g., coordination, electrostatic adsorption, or specific recognition), leading to pronounced changes in optical signals (such as fluorescence quenching, enhancement, or wavelength shifts), thereby enabling highly sensitive detection of analytes.¹¹²

In recent years, a variety of high-performance fluorescent probes have been developed. For example, an organic small-molecule near-infrared probe, NRh6G-FA, constructed by introducing a hemicyanine dye into the rhodamine 6G framework, exhibits rapid response, visible color change, and high sensitivity toward Cu^{2+} , and has been successfully applied in MMs and live-cell imaging (Fig. 6a).⁷⁶ This probe demonstrated excellent selectivity against common interfering ions, with recoveries of 93–107% in MMs matrices (*Astragalus* and *Paeonia lactiflora*), indicating good anti-interference ability and accuracy. Meanwhile, fluorescent nanomaterials have become a key foundation for constructing sensing platforms due to their excellent optical properties and ease of functionalization.^{113,114} A notable example is carbon dots, which achieve fluorescence quenching through specific interactions (e.g., coordination with surface functional groups such as carboxyl groups) with Hg^{2+} , enabling highly

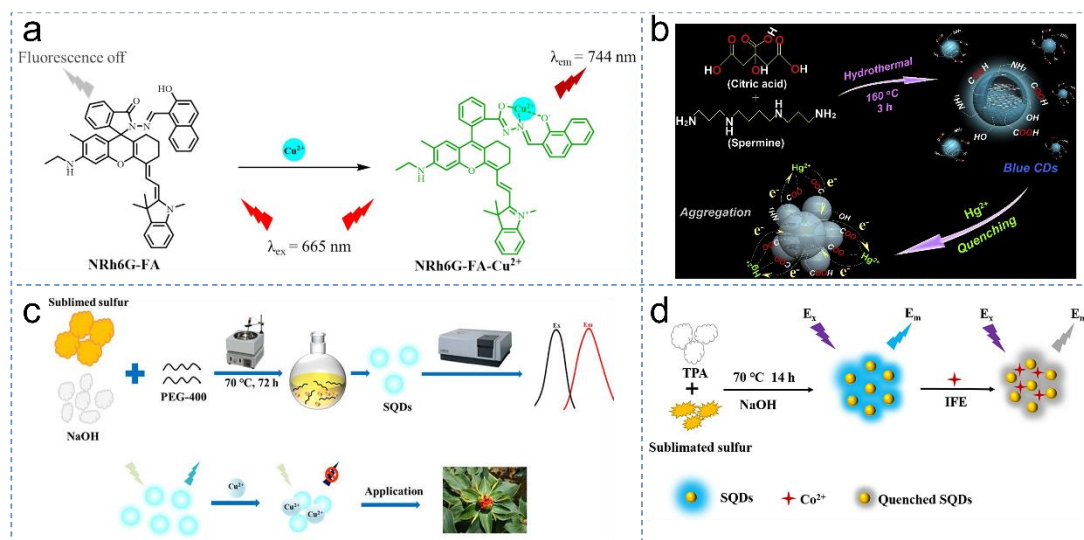


Fig. 6 Schematic of (a) NRh6G-FA applied to the detection of Cu^{2+} in *Astragalus* and *Paonia lactiflora*, “naked eye” identification and bioimaging of Cu^{2+} in living MCF-7 cells (adapted with permission from Ref. ⁷⁶), (b) the one-step hydrothermal synthetic route of carbon dots and electron transfer from carbon dots to Hg^{2+} (adapted with permission from Ref. ⁷⁷), (c) turn-off fluorescent probe of sulfur quantum dots based on inner filter effect for detection of Cu^{2+} residues among *Paris polyphylla* var. *yunnanensis* (adapted with permission from Ref. ⁷⁸), and (d) sulfur quantum dots as fluorescent nanoprobe for Co^{2+} detection in *Salviae miltiorrhizae Radix et Rhizoma* (adapted with permission from Ref. ⁷⁹).

selective detection of trace Hg^{2+} in MMs. This probe exhibited strong selectivity against common interfering ions and achieved 90%–110% recoveries in samples matrix, indicating good accuracy and reliable anti-interference performance in complex MMs. In addition, visual semi-quantitative screening can be realized with the aid of test strips (Fig. 6b).⁷⁷ Sulfur quantum dots, as an emerging class of fluorescent nanoprobe, can be synthesized via “assembly-disassembly” strategies or one-pot methods, and exhibit ultrasmall size, good water solubility, and excellent optical stability. Based on the inner filter effect between sulfur quantum dots and Cu^{2+} or Co^{2+} , rapid and selective fluorescence detection of Cu^{2+} in *Paris polyphylla* var. *yunnanensis* and Co^{2+} in *Salviae miltiorrhizae Radix et Rhizoma* can be achieved, respectively. With LODs at the micromolar level, these systems demonstrate significant potential for direct application in complex MMs matrices (Figs 6c and 6d).^{78,79} To further enhance recognition specificity, fluorescent aptasensors constructed by integrating biological recognition elements (e.g., aptamers) with nanomaterials (such as nitrogen-doped carbon quantum dots) have been developed, enabling detection of Cd^{2+} in *Panax notoginseng*. The designed fluorescent aptamer sensor exhibited strong anti-interference capability and stable performance in complex *Panax notoginseng* samples. Compared with ICP-MS, which can be affected by matrix components such as saponins, the proposed method showed higher stability, detection efficiency, and accuracy.⁸⁰

Although the aforementioned molecular and nanomaterial-

based sensing methods exhibit outstanding performance in terms of selectivity, sensitivity, and on-site applicability, their applications are still largely limited to the detection of single or a few target elements, and their quantitative accuracy in complex real samples is often susceptible to matrix interference. To address this issue, recent studies have adopted effective strategies to circumvent or minimize matrix interference. One common approach is volatile species generation coupled with headspace sampling, which physically separates the target analyte from the interfering liquid matrix. For instance, an arsenic field test kit based on arsine-induced formation of silver nanoparticles on solid-phase fluorescence papers achieves a detection limit of $0.36 \mu\text{g L}^{-1}$ with good selectivity against coexisting ions.¹¹⁵ Similarly, a dairy iodine detection device integrates headspace single-drop microextraction with a ratiometric fluorescence filter effect, achieving 107-fold enrichment and high tolerance to common interferents.²² Another point-of-care platform for urinary iodine uses a solid-phase fluorescence filter effect and headspace introduction, effectively eliminating urine matrix interference with a detection limit of 10 nM.¹¹⁶

These examples demonstrate that combining volatile species generation, headspace separation, and solid-phase or ratiometric detection can dramatically reduce matrix interference. However, for routine quality control of MMs, reproducibility and matrix interference (e.g., from coexisting polyphenols, ions, polysaccharides, or proteins) still require systematic evaluation. Therefore, current research efforts are focused on developing

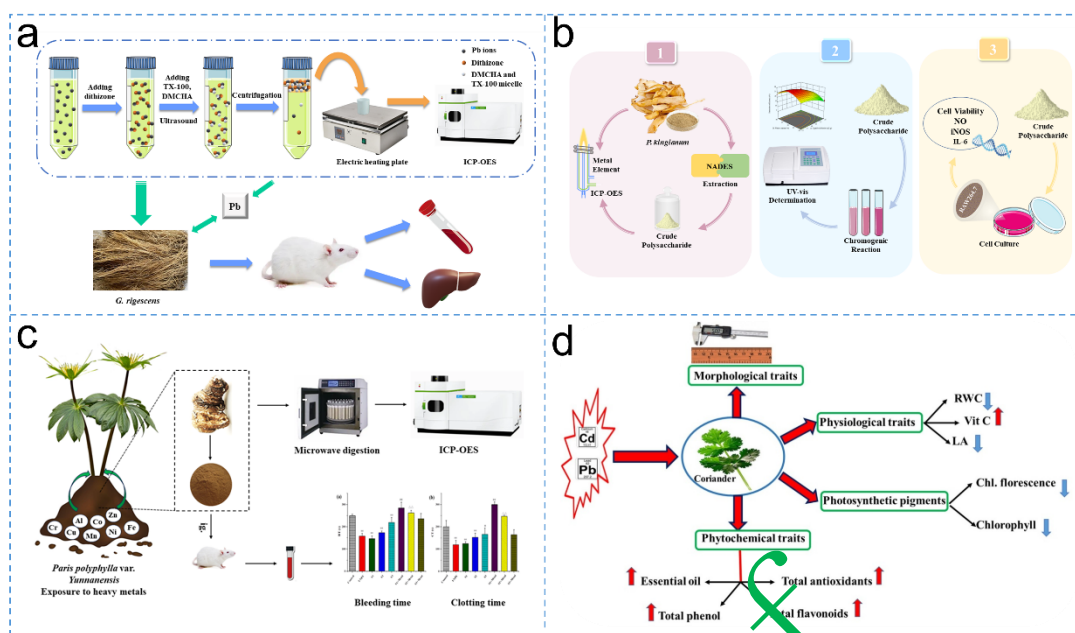


Fig. 7 Schematic diagram of the study on the effects of elements on the pharmacodynamics of (a) *Gentiana rigescens* (adapted with permission from Ref. ¹¹⁹), (b) *Polygonatum kingianum* (adapted with permission from Ref. ¹²⁰), (c) *Paris polyphylla* var. *tsumanensis* (adapted with permission from Ref. ¹²¹), and (d) *Coriandrum sativum* L. (adapted with permission from Ref. ¹²²).

novel multifunctional probes, optimizing recognition interfaces, introducing signal amplification strategies, and promoting integration with portable devices to enhance methodological robustness and real-time on-site detection capabilities. In a nutshell, molecular spectroscopy and nanosensing technologies based on functionalized probes are becoming indispensable tools for the rapid screening, field monitoring, and precise risk assessment of elements in MMs.

APPLICATIONS

Implications of elements on the pharmacodynamics of MMs.

Toxic elements (especially HMs) stress on medicinal plants is not merely an environmental pollution issue, but also a critical factor directly affecting their core medicinal value (pharmacological efficacy). Recent studies (Table 3) have provided in-depth insights into the mechanisms by which HMs interfere with secondary metabolism in medicinal plants and weaken their pharmacological activities.

HM accumulation can significantly alter the biochemical status and active constituents of medicinal plants. Studies have shown that in medicinal plants such as *Holarrhena pubescens* and *Wrightia tinctoria* growing in industrial areas, HM enrichment induces oxidative stress (elevated H_2O_2 and malondialdehyde), accompanied by significant decreases in primary metabolites

(soluble carbohydrates and total proteins) and key secondary metabolites (total phenolics and flavonoids), as well as reduced free radical scavenging activity, directly indicating a decline in their medicinal potential.¹¹⁷ Similarly, *Tussilago farfara* L. growing in urban polluted environments exhibits a substantial reduction in phenolic and flavonoid contents in its leaves, thereby limiting its medicinal applicability.¹¹⁸ These findings confirm that HM contamination can fundamentally impair the quality of medicinal plants by disrupting antioxidant systems and secondary metabolic pathways.

More targeted studies have directly validated the adverse effects of HMs on specific pharmacological activities through “pollution-efficacy” correlation models. This is evidenced by the finding that Pb exposure dose-dependently attenuates the hepatoprotective effects of *Gentiana rigescens* and its active component gentiopicroside in an immunological liver injury mouse model. At higher Pb levels, hepatocyte necrosis and inflammatory infiltration are even exacerbated (Fig. 7a).¹¹⁹ At the cellular level, crude extracts of *Gentiana rigescens* protect H_2O_2 -injured LO2 hepatocytes by regulating the antioxidant enzyme system. However, the presence of moderate levels of mixed metal ions in the decoction attenuates this protective effect.²³ Similarly, *Polygonatum kingianum* crude polysaccharide can activate macrophages and promote the secretion of NO and cytokines at specific concentrations, but their immunomodulatory activity is inhibited when metal element levels exceed the plant’s natural

background values (Fig. 7b).¹²² Furthermore, studies on *Paris polyphylla* var. *Yunnanensis* provide additional evidence supporting this pattern. It was found that the concentrations of various elements (e.g., Cu, Ni, Mn, and Zn) in *Paris polyphylla* var. *Yunnanensis* are significantly higher than those in its crude extracts. When a mixture of elements at levels comparable to those in *Paris polyphylla* var. *Yunnanensis* was co-administered with the crude extract in mice, the original hemostatic effect was markedly inhibited (Fig. 7c).¹²¹ These experiments unequivocally demonstrate that even when elements concentrations do not reach levels associated with acute toxicity, they are still sufficient to antagonize or weaken the core therapeutic functions of medicinal plants.

Moreover, the effects of HM stress on pharmacologically active components exhibit a complex “dual nature”. On the one hand, in *Coriandrum sativum* L., exposure to Cd and Pb stress can lead to increases in total phenolic and flavonoid contents, as well as essential oil yield (Fig. 7d).¹²² *Coriandrum sativum* L. exposed to Zn and Cu stress exhibits enhanced antioxidant or antimicrobial activity in its extracts. This suggests that, under certain conditions, HMs may act as elicitors, inducing plants to produce defensive secondary metabolites. However, such changes in constituent levels do not necessarily translate into desirable or safe pharmacological effects. For instance, *Lavandula dentata* L. grown under Cd and Pb stress exhibits enhanced cytotoxicity in its leaf extracts, potentially indicating a fundamental alteration in its medicinal properties.¹²³ This diversity in “stress-response” relationships suggests that the impact of HMs on pharmacological efficacy is the result of a complex interplay among dosage, metal species, plant type, and target pharmacological activity, and therefore cannot be simply generalized as either “promotion” or “inhibition”.

Currently, direct human studies linking elemental composition to patient-relevant outcomes—such as symptom relief, recovery time, or adverse event rates—are still lacking. Future research should integrate elemental analysis with clinical pharmacovigilance data and conduct dose-response trials to establish evidence-based safety and efficacy thresholds for essential and toxic elements in MMs, thereby bridging the gap between analytical chemistry and clinical practice.

Element migration behavior in the “soil-medicinal plant” system. In the “soil-medicinal plant” system, the concentration of toxic elements (especially HMs) serves as a key indicator for assessing soil contamination levels, while their transfer and accumulation from soil to plants are of great significance for evaluating the quality and safety of medicinal plants and mitigating associated health risks. Table 3 summarizes the applied research on elemental migration behavior in the “soil-medicinal plant” system. By employing the bioconcentration factor and translocation factor, researchers have evaluated the migration

capacity of multiple elements, including Al, Fe, Mn, Cu, Pb, Zn, Cr, As, and Cd, in the soil-*Paeonia Lactiflora* Pall. system in Bozhou, Anhui Province, China, as well as the transfer behavior of Hg, Cd, As, Pb, and Cu in the “soil-*Gastrodia elata*” system in its main production areas in Yunnan. Additionally, indices such as the geoaccumulation index, pollution load index, and potential ecological risk index have been applied to assess soil HM contamination. The results indicate that Fe, Mn, Cr, and As are the priority pollutants in the habitat soil of the *Paeonia Lactiflora* Pall. And it exhibits a high potential to transfer Zn, Cu, and Fe from soil to roots. Except for Cd, other HMs show strong translocation capability from roots to stems and leaves.¹²⁴ In the habitat soil of *Gastrodia elata*, the pollution levels of five HMs follow the order Hg>Cd>Cu>As>Pb, with Hg, Cd, and Cu reaching severe contamination levels. The accumulation capacity of *Gastrodia elata* for soil HMs is ranked as Hg>Cd>As>Pb>Cu.¹²⁵

The migration behavior of HMs is jointly influenced by their chemical speciation, soil properties, and plant species in the “soil-medicinal plant” system. Studies on *Epimedium* and *Houttuynia cordata* Thunb. have shown that HMs predominantly exist in the residual state in soils, while the more bioavailable forms, such as water-soluble and ion-exchangeable states, are present at lower levels, though their contribution to plant uptake remains non-negligible. *Epimedium* leaves exhibit strong accumulation capacities for Cr, Ni, Cu, As, and Pb, whereas roots preferentially accumulate Zn, indicating organ-specific distribution patterns of HMs within plants. At the mechanistic level, the root system acts as a selective barrier: toxic elements like As and Pb are largely rejected by *Epimedium* roots, with only a small fraction entering the plant. This protective mechanism involves multiple factors: (1) root secretions form complex colloids that reduce trace element bioavailability in the soil; (2) root/mycorrhizal structures restrict the entry of elements into the xylem; (3) heavy metals that enter root cells are predominantly in the reduced state (e.g., Cu), whereas the bioeffective fraction in soil exists mainly in the oxidized state (e.g., Cu²⁺); and (4) cell walls, particularly suberin proteins in the endodermal and exodermal cell walls, act as barriers controlling water and ion uptake, thereby limiting the accumulation and transport of excess heavy metals such as Cr, Ni, Pb, and Cd from soil to roots. Furthermore, the organic bound state, ion exchange state, and active state of HMs in soil significantly influence their concentrations in different parts of *Epimedium*, indicating that, in addition to labile forms, other fractions also participate in the migration process.¹²⁶ In the *Houttuynia cordata* Thunb. system, soil HMs such as Zn, Cu, Mn, and Co can affect the availability of nutrients, including available phosphorus, available potassium, and organic matter, thereby indirectly regulating the quality of MMs. The migration capacity of HMs varies among elements; Cr exhibits strong translocation to stems and leaves, while Fe also shows a tendency for upward transport. Notably, Cr, Pb, and Cu exhibit relatively high contamination levels in *Houttuynia cordata* Thunb. Although Pb and Cu remain

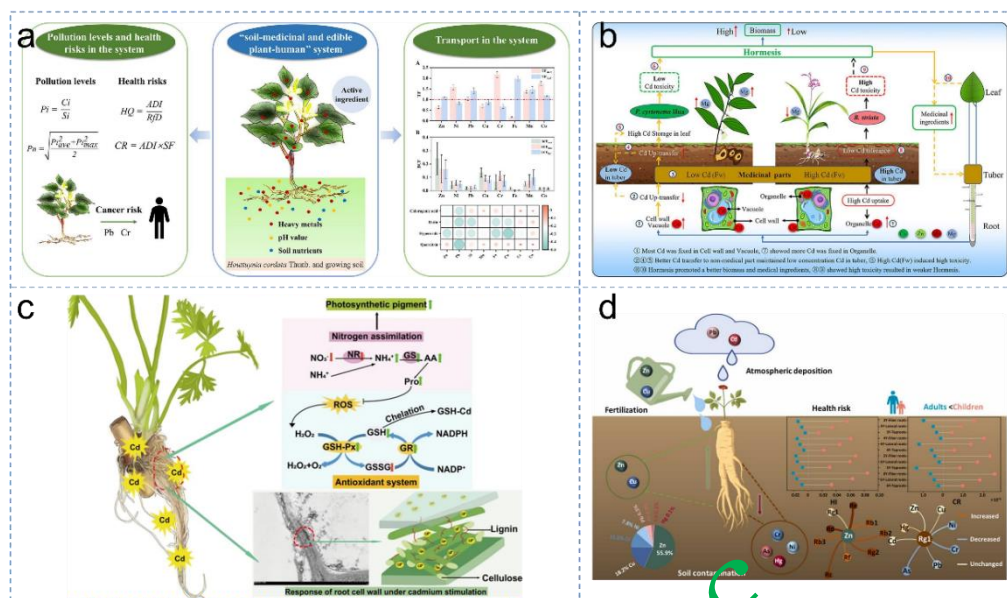


Fig. 8 Schematic of the study on the comparative migration behavior of elements in the (a) “soil-*Houttuynia cordata* Thunb.” (adapted with permission from Ref. ¹²⁷), (b) “soil-*Polygonatum cyrtoneuma* Hua” (adapted with permission from Ref. ¹²⁸), (c) “soil-*Zastisium sinense* cv. Chuanxiong” (adapted with permission from Ref. ¹³¹), and (d) “soil-*Panax ginseng*” systems (adapted with permission from Ref. ¹³²).

within acceptable limits, they still pose potential carcinogenic risks, highlighting the necessity of considering synergistic HM migration and health risk assessment when cultivating medicinal plants in regions with high background levels (Fig. 8a).¹²⁷

In the context of the safe utilization of Cd-contaminated soils, studies on two rhizomatous medicinal plants, *Polygonatum cyrtoneuma* Hua and *Bletilla striata*, have revealed distinct Cd migration and detoxification mechanisms. Under Cd stress at 0.91 mg kg⁻¹, the Cd content in *Polygonatum cyrtoneuma* Hua remained below the limit specified in the Chinese Pharmacopoeia (1 mg kg⁻¹), whereas *Bletilla striata* was only considered safe in control soil with 0.25 mg kg⁻¹ Cd, indicating that the former exhibits superior Cd tolerance. The underlying mechanism lies in the fact that the former can immobilize most Cd in the roots and efficiently translocate it to non-medical parts (aboveground tissues). Additionally, more than 80% of Cd is compartmentalized within the cell wall and vacuoles, significantly reducing its toxicity to organelles. In contrast, Cd in the latter tends to accumulate in organelles, with a higher proportion of bioavailable water-soluble Cd, resulting in inhibited growth. Notably, low concentrations of Cd (0.91 mg kg⁻¹) exhibit a hormetic effect on both medicinal plants, promoting biomass accumulation while enhancing the contents of pharmacologically active constituents such as ethanol-soluble extractives, phenolics, flavonoids, and saponins. Furthermore, the former exhibits synergistic uptake of Cd and mineral elements (Zn, Mn, and Mg), which contributes to maintaining photosynthetic capacity and stress resistance. A comprehensive evaluation model based on the analytic hierarchy

process further confirms that *Polygonatum cyrtoneuma* Hua poses a relatively low cultivation risk in soils with Cd concentrations ≤ 0.91 mg kg⁻¹, whereas *Bletilla striata* requires soils with lower Cd levels (Fig. 8b).¹²⁸

Similar findings in *Panax notoginseng* also support the hormetic effect of Cd. When the soil Cd concentration reaches 1 mg kg⁻¹, *Panax notoginseng* exhibits peak Cd accumulation, accompanied by increased biomass and elevated saponin content; however, higher Cd levels inhibit plant growth and metabolism. In addition, the effects of Cd on the rhizosphere microenvironment are dose-dependent: under low Cd stress, the abundance of specific rhizosphere microbial populations increases, whereas under high Cd stress, microbial diversity declines and Cd-tolerant species become dominant.¹²⁹ At the molecular level, low Cd concentrations induce oxidative stress in plants, increase signaling molecules, upregulate the expression of antioxidant enzyme genes, and enhance the production of secondary metabolites such as saponins. Metals entering plant tissues may regulate secondary metabolite expression through two mechanisms: (1) binding to specific proteins involved in electron transfer (e.g., chlorophyll-binding proteins, carbonic anhydrase, Rubisco) to enhance photosynthesis, thereby increasing sugar and energy availability for secondary metabolite synthesis; and (2) interfering with the cellular antioxidant system, triggering reactive oxygen species as direct signaling molecules or activating other signaling pathways, which enhances enzyme gene expression and ultimately elevates secondary metabolite content. Furthermore, the hormetic effect in *Panax notoginseng* is mediated by plant-microbe interactions: low

Cd concentrations activate the plant's tolerance system, altering the soil environment via root exudates and recruiting beneficial microorganisms (e.g., Rhizobiaceae, Streptomycetaceae, Mesorhizobium) that enhance nutrient cycling, release plant hormones, and boost defense enzyme activity. The cell wall acts as an initial barrier, and root/mycorrhizal structures restrict Cd entry into the xylem, with suberin proteins in endodermal cell walls controlling ion uptake. These molecular and transport protein-level mechanisms collectively underlie the dose-dependent hormetic response observed in *Panax notoginseng*.

At the subcellular and molecular levels, studies on *Ligusticum sinense cv. Chuanxiong* have elucidated the mechanisms of Cd accumulation and detoxification. Cd is predominantly accumulated in root cell walls and is closely associated with cell wall thickening, increased cellulose content, and glutathione-mediated chelation. Transcriptomic analysis further indicates that Cd stress significantly upregulates the expression of Cd transport-related genes (e.g., NRAMP5, CAX3, YSL7) as well as key transcription factors (e.g., BHLH162, ERF109). The roots of *Ligusticum sinense cv. Chuanxiong* achieve a balance between growth and stress resistance through multiple pathways, including carbon metabolism, sulfur metabolism (a core detoxification pathway), and phenylpropanoid biosynthesis (Fig. 8c).^{130,131} As one of the most valuable herbal medicines and functional foods worldwide, *Panax ginseng* has attracted considerable attention regarding the relationship between HM translocation and the accumulation of bioactive constituents across its different tissues. Studies on 3–6-year-old *Panax ginseng* indicate that the accumulation of ginsenosides (nine types, including Rg, Rb1, Rc, and Rg1) increases with cultivation age, with the highest levels found in fibrous roots, followed by lateral roots and main roots. Meanwhile, the average residual concentration of eight HMs (Cu, Zn, Ni, Cr, Pb, As, Cd, and Hg) also show an increasing trend over time, with Zn exhibiting the highest levels (14.61–53.75 mg kg⁻¹), followed by Cu (8.50–12.49 mg kg⁻¹). Correlation analysis reveals that Zn plays a key role in ginsenoside biosynthesis, showing significant positive correlations with multiple ginsenosides, whereas Cu, Cd, and Hg exhibit weaker or negative effects. Notably, the accumulation of Ni, Cr, Pb, and As may lead to a reduction in ginsenoside Rg1 content. At the molecular level, Zn and Cu act as cofactors for farnesyl-pyrophosphate synthase, a key enzyme in the isoprenoid pathway that produces ginsenoside precursors. Cd²⁺ shares similar chemical properties with Zn²⁺ and Ca²⁺, leading to its accidental uptake by root transport proteins. Cr easily penetrates cell membranes via the sulfate pathway, causing DNA damage. These transport protein-mediated mechanisms underlie the observed correlations between specific heavy metals and ginsenoside accumulation. Dietary risk assessment indicates that the health risk index associated with ginseng consumption is generally higher in children than in adults, highlighting the need for particular attention to potential exposure risks in pediatric populations (Fig. 8d).¹³²

In a nutshell, the migration behavior of heavy metals in the “soil-medicinal plant” system is synergistically regulated by metal speciation, soil physicochemical properties, and plant species, exhibiting significant organ-specific distribution patterns and interspecific differences. Under low-concentration heavy metal stress, some plants can achieve detoxification through mechanisms such as cell wall compartmentalization and chelation, even displaying a hormetic effect (low-dose stimulation, high-dose inhibition), whereas high-concentration stress suppresses growth and affects the accumulation of bioactive constituents. Therefore, an in-depth understanding of the migration patterns and detoxification mechanisms is of great value for scientifically guiding the selection of cultivation areas for medicinal plants, ensuring the quality and safety of MMs, and refining risk assessment systems based on migration behavior.

Human health risk assessment from MMs consumption. In the safety evaluation system of medicinal plants, human health risk assessment based on HM detection data has become an indispensable core component (Table 3). At present, internationally accepted assessment models are mainly based on methods recommended by the USEPA. Non-carcinogenic risk is evaluated by calculating the EDI, THQ, and HI, while CR is used to quantify the lifetime probability of cancer. Global assessment studies indicate that although the concentrations of certain HMs in medicinal plants from many regions may exceed the limits recommended by the WHO, the THQ and HI values calculated based on conventional exposure models are generally below the safety thresholds, suggesting that the non-carcinogenic health risks associated with long-term consumption are overall controllable.¹³³

For example, analyses of commercially available solid and liquid herbal preparations have shown that both the total non-carcinogenic risk and total carcinogenic risk are well below the recommended limits set by the USEPA;¹³⁴ comprehensive assessments of various medicinal plants have likewise indicated that the chronic non-carcinogenic health risks posed by HMs are acceptable.¹³⁵ However, the risks under specific contaminated environments should not be overlooked. In mining areas of Ghana, the concentrations of Cr, Cd, and Pb in medicinal plants generally exceed permissible limits.¹³⁶ Specifically, one study reported that *Paullinia pinnata* recorded the highest Cd concentration, which was about 447% above the WHO maximum permissible limit of 0.30 mg kg⁻¹; *Newbouldia laevis* yielded the highest Cr concentration, about 507% above the WHO maximum permissible limit; and for Pb, *Alchornea cordifolia* recorded the highest mean concentration, 264.1% greater than the WHO maximum permissible limit. Similarly, in industrial and mining regions of Turkey, HM levels in medicinal plants are slightly higher than the WHO limits.¹³⁷ Of particular concern, a systematic assessment of *Panax notoginseng* revealed that analysis of 69 topsoil and 10 *Panax notoginseng* samples from Yunnan showed slight soil pollution (Nemerow index 1.8), with an average HI of

1.29 and As CR exceeding the threshold, posing health risks to growers. The *Panax notoginseng* was polluted by Cd, As, and Pb. Moreover, 39.1% of estimated daily intakes of As for consumers through leaf consumption exceeded the permitted daily exposure, suggesting a potential health risk.¹³⁸ The accuracy of risk assessment is highly dependent on understanding the bioaccessibility and chemical speciation of HMs. A case in point is *Cordyceps sinensis*: although its total As content is relatively high, its bioaccessibility under simulated gastrointestinal conditions is approximately 64.5%. Speciation analysis based on HPLC-ICP-MS further indicates that the highly toxic inorganic As accounts for only 8.69% of the total As, resulting in a significantly reduced health risk after correction.¹³⁹ This highlights the importance of incorporating bioaccessibility correction for the objective evaluation of the safety of medicinal plants, particularly mineral medicines and those with high background levels.

Current research frontiers are moving toward more precise risk assessment. On the one hand, *in vitro* simulated digestion models are being integrated with cellular uptake models to determine the bioaccessibility and bioavailability of HMs, and to refine intake data accordingly, thereby enabling assessments that more closely reflect real exposure scenarios.¹⁴⁰ On the other hand, considering the multi-component co-exposure characteristics of MM, cumulative risk assessment models based on target organ toxicity have been developed. This is illustrated by the application of the HI method to evaluate the cumulative risk of several MMs by accounting for the combined exposure to Pb, Cd, and As, as well as the effects of the decoction process. The results indicate that, after incorporating bioavailability and preparation methods, the health risks remain within acceptable levels.¹⁴⁰ These advances indicate that future health risk assessments will become increasingly refined and dynamic. They will evolve from simple total concentration comparisons to integrated evaluation frameworks. Such frameworks incorporate advanced analytical techniques (*e.g.*, speciation analysis), toxicological data, and realistic human exposure patterns. As a result, they will provide a more robust scientific basis for the safe use and regulation of medicinal plants.

CONCLUSION

Elemental analysis of MMs is a multidisciplinary and rapidly evolving field. This review systematically summarizes recent advances spanning green sample pretreatment, advanced analytical detection, and final health risk assessment. In terms of methodology, green solvents represented by DES and their switchable variants are revolutionizing conventional digestion and extraction processes, enabling efficient matrix disruption and selective analyte enrichment under mild conditions while significantly reducing the use of hazardous chemicals and waste

generation. The development of solid-phase microextraction techniques, particularly novel adsorbents based on functionalized magnetic materials, has not only enhanced the sensitivity and selectivity of trace elemental analysis but also expanded their application to the selective removal of toxic HMs from MMs decoctions, reflecting a functional extension from “analytical detection” to “decontamination treatment”. Analytical techniques exhibit a diversified and complementary landscape: highly sensitive ICP-MS coupled with speciation analysis serves as the “gold standard” for precise laboratory quantification; simple, cost-effective AAS, AFS, and ICP-OES remain indispensable for routine monitoring; LIBS, XRF, and portable fluorescence sensing technologies offer unique advantages for on-site rapid screening and spatial distribution analysis; while non-destructive or minimally destructive nuclear analytical techniques play a critical role as authoritative reference methods in certified reference material value assignment and method validation.

Concurrently, research understanding has deepened from simplistic “total content control” toward an integrated understanding of how elements influence the pharmacodynamics of MMs, as well as their migration and transformation within the “soil-medicinal plant” system. The chemical speciation of elements, soil physicochemical properties, and plant uptake and transport characteristics collectively determine their accumulation levels in MMs. Further studies have revealed that HM stress can interfere with secondary metabolic pathways through oxidative stress, directly diminishing or altering the intrinsic pharmacological activity of medicinal plants, while under certain conditions it may also induce defense responses and modify the profile of bioactive constituents. This dualistic and complex “stress-response” relationship indicates that assessing the impact of HMs on the quality of MMs must transcend simple determinations of content exceedances, instead integrating speciation analysis, migration patterns, and pharmacodynamic evaluations. In health risk assessment, traditional models are based on total content. However, these models are now being supplemented and refined by more precise approaches. These approaches include: (1) elemental chemical speciation analysis, (2) *in vitro* bioaccessibility and bioavailability assays, and (3) target organ toxicity-based cumulative risk assessment models. By integrating these methods, we can more realistically reflect the actual health risks posed by heavy metal intake from medicinal plants. This integration also provides a basis for establishing more scientifically sound regulatory limits and risk management strategies.

CHALLENGES AND FUTURE PERSPECTIVES

Nevertheless, several limitations persist in current research. At the

methodological level, the universal digestion mechanisms of green solvents for complex MM matrices-especially animal-derived and mineral drugs-remain unclear, and their online coupling with high-throughput detection platforms still requires advancement. Regarding mechanistic understanding, the specific molecular interactions between elements and bioactive constituents, synergistic or antagonistic effects under combined contamination, and the dynamic transformation patterns of elemental speciation during processing and preparation remain to be systematically elucidated. In risk assessment, bioaccessibility data remain scarce, existing studies predominantly focus on single elements, and systematic evaluation of multi-element co-exposure is lacking, while the correlation between in vitro models and actual human absorption requires further validation.

Looking ahead, future research in this field is expected to advance in the following directions: firstly, the intelligentization and standardization of methodologies, developing universal green pretreatment platforms suitable for diverse MM categories, promoting artificial intelligence-assisted optimization of analytical conditions, and establishing standardized operating procedures and inter-laboratory comparison systems for various analytical techniques. Secondly, the deep integration of source apportionment (i.e., the quantitative identification and allocation of elemental sources) with migration and transformation studies, utilizing multi-isotope tracer techniques to quantitatively elucidate the contributions of element sources and their migration pathway. Thirdly, the mechanistic elucidation of combined contamination, constructing pharmacodynamic-toxicity evaluation models for multi-element co-exposure and systematically investigating the interactions between HMs and bioactive constituents in MMs. Fourthly, precision risk assessment, establishing a full cycle risk monitoring network covering “production environment-cultivation/processing-clinical application”, integrating high-throughput speciation analysis, bioaccessibility databases, and artificial intelligence-based early warning models to construct a dynamic, intelligent risk assessment system that provides comprehensive technical support for the green production and safe application of MMs.

AUTHOR INFORMATION

Xiaodong Wen is XXX

Shengchun Yang is XXX

Corresponding Author

* X. D. Wen

Email address: wenxiaodong@dali.edu.cn

* S. C. Yang

Email address: yangshengchun@dali.edu.cn

These authors contributed equally to this work and share first authorship.

Notes

The authors declare that they have no known competing financial interests or personal relationships that could have appeared to influence the work reported in this paper.

ACKNOWLEDGMENTS

The authors would like to gratefully acknowledge the National Natural Science Foundation of China (22176021), Yunnan Fundamental Research Projects (202401AS070028), and Yunnan Provincial Department of Education Scientific Research Fund Project (2026J0865).

REFERENCES

1. W. Chen, Y. Yang, K. Fu, D. Zhang, and Z. Wang, *Front. Pharmacol.*, 2022, **13**, 891273. <https://doi.org/10.3389/fphar.2022.891273>
2. C. Guo, L. Lv, Y. Liu, M. Ji, E. Zang, Q. Liu, M. Zhang, and M. Li, *Crit. Rev. Anal. Chem.*, 2023, **53**, 339–359. <https://doi.org/10.1080/10408347.2021.1953371>
3. N. Khan, N. Jamila, F. Amin, R. Masood, A. Atlas, W. Khan, N. U. Ain, and S. N. Khan, *Arab. J. Chem.*, 2021, **14**, 103055. <https://doi.org/10.1016/j.arabjc.2021.103055>
4. X. Zhong, Z. Di, Y. Xu, Q. Liang, K. Feng, Y. Zhang, L. Di, and R. Wang, *Chin. Med-UK*, 2022, **17**, 21. <https://doi.org/10.1186/s13020-022-00577-9>
5. O. Acar, A. Tunçeli, and A. R. Türker, *Food Anal. Method*, 2016, **9**, 3201–3208. <https://doi.org/10.1007/s12161-016-0516-4>
6. G. K. Deshwal, L. G. Gómez-Mascaraque, M. Fenelon, and T. Huppertz, *Molecules*, 2023, **28**, 3988. <https://doi.org/10.3390/molecules28103988>
7. W. Zhou, M. N. Wiczorek, H. Javanmardi, and J. Pawliszyn, *TrAC, Trends Anal. Chem.*, 2023, **166**, 117167. <https://doi.org/10.1016/j.trac.2023.117167>
8. S. Armenta, S. Garrigues, F. A. Esteve-Turrillas, and M. de la Guardia, *TrAC, Trends Anal. Chem.*, 2019, **116**, 248–253. <https://doi.org/10.1016/j.trac.2019.03.016>
9. C. M. Hussain, G. Hussain, and R. Keçili, *TrAC, Trends Anal. Chem.*, 2025, **191**, 118295. <https://doi.org/10.1016/j.trac.2025.118295>
10. H. Wang, Y. Zhang, W. Bi, and D. D. Y. Chen, *TrAC, Trends Anal. Chem.*, 2026, **198**, 118736. <https://doi.org/10.1016/j.trac.2026.118736>
11. W. O. Santos, L. C. Corrêa-Filho, L. Melo, A. H. Oliveira, S. Pacheco, L. M. C. Cabral, B. D. Ribeiro, and R. V. Tonon, *Food Chem.*, 2026, **507**, 148276. <https://doi.org/10.1016/j.foodchem.2026.148276>
12. J. Jiang, L. Shen, F. Xu, L. Liu, J. Li, Q. Xu, Z. Li, and H. Qiu, *Chinese Chem. Lett.*, 2026, 112412. <https://doi.org/10.1016/j.ccllet.2026.112412>

13. R. Yang, Q. Li, W. Zhou, S. Yu, and J. Liu, *Anal. Chem.*, 2022, **94**, 16328–16336. <https://doi.org/10.1021/acs.analchem.2c03018>
14. E. Chajduk and H. Polkowska-Motrenko, *Food Chem.*, 2019, **292**, 129–133. <https://doi.org/10.1016/j.foodchem.2019.04.051>
15. R. Zhang, S. Hu, C. Ma, T. Zhang, and H. Li, *TrAC, Trends Anal. Chem.*, 2024, **181**, 117992. <https://doi.org/10.1016/j.trac.2024.117992>
16. S. Liu, Y. Wang, Z. Wang, L. Zhang, C. Niu, H. Ma, W. Yang, and L. Guo, *Talanta*, 2026, **304**, 129539. <https://doi.org/10.1016/j.talanta.2026.129539>
17. Z. Q. Zhou, X. Zhou, J. Sun, Y. Tang, J. Wang, and K. S. Yao, *Atom. Spectrosc.*, 2026, **47**, 122–140. <https://doi.org/10.46770/AS.2025.262>
18. M. Zhang, J. Hu, Q. Tang, J. Zhang, X. Jiang, and X. Hou, *Anal. Chem.*, 2023, **95**, 14169–14174. <https://doi.org/10.1021/acs.analchem.3c01130>
19. Y. Li, J. Hu, C. Li, and X. Hou, *Anal. Chem.*, 2024, **96**, 5757–5762. <https://doi.org/10.1021/acs.analchem.4c00063>
20. X. Yu, X. B. Su, W. R. Song, B. P. Li, D. Zhao, R. Yang, Z. Y. Hou, and Z. Wang, *Atom. Spectrosc.*, 2026, **47**, 1–12. <https://doi.org/10.46770/AS.2025.279>
21. Z. Zhang, Y. Liu, Y. Lin, J. Zhang, and C. Zheng, *TrAC, Trends Anal. Chem.*, 2026, **195**, 118552. <https://doi.org/10.1016/j.trac.2025.118552>
22. R. Gao, S. Ye, X. Yang, Y. Zhang, Y. Liu, J. Zhang, and C. Zheng, *Food Chem.*, 2025, **484**, 144418. <https://doi.org/10.1016/j.foodchem.2025.144418>
23. X. Yang, C. Yan, R. Zhang, Y. Sun, Z. Li, Y. Liu, S. Yang, L. Shen, and X. Wen, *Anal. Chim. Acta*, 2022, **1221**, 340109. <https://doi.org/10.1016/j.aca.2022.340109>
24. X. Liu, X. Yang, Y. Sun, F. Ji, M. Guo, D. He, J. Hu, F. Hao, K. Hu, and X. Wen, *Food Chem.*, 2025, **492**, 145538. <https://doi.org/10.1016/j.foodchem.2025.145538>
25. M. Aghamohammadi, M. Faraji, P. Shahdousti, H. Kalthor, and A. Saleh, *Phytochem. Anal.*, 2015, **26**, 209–214. <https://doi.org/10.1002/pca.2554>
26. D. He, X. Yang, J. Hu, H. Chi, N. Lu, Y. Liu, K. Hu, S. Yang, and X. Wen, *Microchem. J.*, 2024, **196**, 109637. <https://doi.org/10.1016/j.microc.2023.109637>
27. F. Ji, T. Xu, X. Yang, Y. Zhao, H. Huang, F. Hao, X. Yu, and X. Wen, *Microchem. J.*, 2026, **221**, 116707. <https://doi.org/10.1016/j.microc.2025.116707>
28. T. Xia, X. Yang, D. He, X. Liu, H. Chi, Y. Liu, S. Yang, and X. Wen, *Microchem. J.*, 2022, **179**, 107632. <https://doi.org/10.1016/j.microc.2022.107632>
29. X. Yang, C. Yan, Y. Sun, Y. Liu, S. Yang, Q. Deng, and X. Wen, *Microchem. J.*, 2021, **168**, 106402. <https://doi.org/10.1016/j.microc.2021.106402>
30. Y. Sun, X. Yang, R. Zhang, T. Xia, K. Hu, F. Hao, Y. Liu, Q. Deng, S. Yang, and X. Wen, *Microchem. J.*, 2023, **187**, 108372. <https://doi.org/10.1016/j.microc.2022.108372>
31. M. M. A. Campos, H. Tonuci, S. M. Silva, B. de S. Altoé, D. de Carvalho, E. A. M. Kronka, A. M. S. Pereira, B. W. Bertoni, S. de C. França, and C. E. S. Miranda, *Phytochem. Anal.*, 2009, **20**, 445–449. <https://doi.org/10.1002/pca.1145>
32. Y. Sun, X. Yang, J. Hu, F. Ji, H. Chi, Y. Liu, K. Hu, F. Hao, and X. Wen, *Talanta*, 2024, **274**, 126036. <https://doi.org/10.1016/j.talanta.2024.126036>
33. Y. Liu, X. Yang, J. Hu, N. Lu, D. He, H. Chi, Y. Liu, S. Yang, and X. Wen, *Anal. Chim. Acta*, 2024, **1290**, 342197. <https://doi.org/10.1016/j.aca.2023.342197>
34. T. Xia, X. Yang, R. Zhang, A. Huang, K. Hu, F. Hao, Y. Liu, Q. Deng, S. Yang, and X. Wen, *Talanta*, 2023, **256**, 124316. <https://doi.org/10.1016/j.talanta.2023.124316>
35. R. Zhang, X. Yang, D. He, Y. Liu, Y. Zhu, Z. Li, Y. Liu, Q. Deng, S. Yang, and X. Wen, *J. Anal. Atom. Spectrom.*, 2022, **37**, 1730–1737. <https://doi.org/10.1039/D2JA00130F>
36. Q. Han, F. Liu, C. Wang, Z. Tang, C. Peng, and Y. Tan, *Arabian J. Chem.*, 2023, **16**, 104635. <https://doi.org/10.1016/j.arabjc.2023.104635>
37. G. C. Costa, A. S. dos Santos, R. G. O. Araujo, M. G. A. Korn, and R. M. M. Santana, *Food Chem.*, 2025, **477**, 143460. <https://doi.org/10.1016/j.foodchem.2025.143460>
38. J.-Y. Cai, H. Shen, J.-N. Xu, J.-M. Xu, J.-H. Wang, and Y.-L. Yu, *Anal. Chem.*, 2025, **97**, 2899–2905. <https://doi.org/10.1021/acs.analchem.4c05556>
39. X. Yang, J. Yang, Y. Su, Y. Deng, X. Wen, and C. Zheng, *Anal. Chem.*, 2025, **97**, 1977–1982. <https://doi.org/10.1021/acs.analchem.4c05740>
40. J.-Y. Cai, X. Zhang, J.-J. Wei, S. Chen, Y.-L. Yu, and J.-H. Wang, *Anal. Chem.*, 2024, **96**, 3733–3738. <https://doi.org/10.1021/acs.analchem.3c05330>
41. X. Yang, C. Yan, Y. Sun, Y. Liu, S. Yang, Q. Deng, Z. Tan, and X. Wen, *TrAC, Trends Anal. Chem.*, 2022, **149**, 116555. <https://doi.org/10.1016/j.trac.2022.116555>
42. M. Haddad, M. Tarahi, D. J. McClements, and F. Aghababaei, *Carbohydr. Polym.*, 2025, **362**, 123683. <https://doi.org/10.1016/j.carbpol.2025.123683>
43. Y. Yan, L. Shen, Y. Wang, B. Gong, Z. Li, and H. Qiu, *Chinese Chem. Lett.*, 2025, **36**, 110845. <https://doi.org/10.1016/j.ccllet.2025.110845>
44. Y. Liu, X. Liu, R. Li, Y. Feng, H. Zhang, and Y. Liang, *Food Chem.*, 2025, **495**, 146230. <https://doi.org/10.1016/j.foodchem.2025.146230>
45. J. Werner, J. Plotka-Wasyłka, N. Jatkowska, S. H. Hashemi, and M. Kaykhaii, *TrAC, Trends Anal. Chem.*, 2026, **194**, 118535. <https://doi.org/10.1016/j.trac.2025.118535>
46. K. Javar, A. Foroozandeh, M. Souiri, H. S. Amoli, and M. Hasanzadeh, *TrAC, Trends Anal. Chem.*, 2025, **185**, 118163. <https://doi.org/10.1016/j.trac.2025.118163>
47. S. E. Bodur, H. Serbest, and S. Bakirdere, *Food Chem.*, 2025, **487**, 144790. <https://doi.org/10.1016/j.foodchem.2025.144790>
48. W. A. Khan, S. A. Hossein Fallah, S. Moltajihagh, F. Hamdi, F. Alipour, A. Mollahosseini, and G. Boczkaj, *TrAC, Trends Anal. Chem.*, 2025, **189**, 118247. <https://doi.org/10.1016/j.trac.2025.118247>
49. Ü. C. ErİM, *Food Chem.*, 2025, **489**, 144996. <https://doi.org/10.1016/j.foodchem.2025.144996>
50. N. Wang, Y. Tian, X. Wu, H. Liu, H. Lu, and Y. Zhu, *ACS Sustainable Chem. Eng.*, 2025, **13**, 9087–9097. <https://doi.org/10.1021/acssuschemeng.5c01837>
51. M. Á. Aguirre, L. Vidal, M. Ahmadi, and A. Canals, *TrAC, Trends Anal. Chem.*, 2025, **189**, 118267. <https://doi.org/10.1016/j.trac.2025.118267>
52. L. B. Santos, A. S. Melo, M. J. Santos, A. M. Santos, S. L. C. Ferreira, and V. A. Lemos, *TrAC, Trends Anal. Chem.*, 2024, **175**, 117738. <https://doi.org/10.1016/j.trac.2024.117738>
53. S. Chen, J. Yan, Y. Liu, C. Wang, and D. Lu, *Food Chem.*, 2021, **359**, 129958. <https://doi.org/10.1016/j.foodchem.2021.129958>

54. Y. W. Yang, J. Liu, J. Huang, C. R. Zhang, S. J. Xiao, X. X. Shao, H. Wu, and L. Zhang, *J. Environ. Chem. Eng.*, 2025, **13**, 118638. <https://doi.org/10.1016/j.jece.2025.118638>
55. F. Uzcan, O. Kaya, and M. Soylak, *Food Chem.*, 2026, **498**, 147285. <https://doi.org/10.1016/j.foodchem.2025.147285>
56. R. Chizzola, H. Michitsch, and C. Franz, *Eur. Food Res. Technol.*, 2003, **216**, 407–411. <https://doi.org/10.1007/s00217-003-0675-6>
57. A.-W. O. El-Rjoob, A. M. Massadeh, and M. N. Omari, *Environ. Monit. Assess.*, 2008, **140**, 61–68. <https://doi.org/10.1007/s10661-007-9847-3>
58. M. U. Khan, M. Adeel, and R. N. and Malik, *Hum. Ecol. Risk Assess.*, 2015, **21**, 1782–1792. <https://doi.org/10.1080/10807039.2014.977744>
59. H. Okatch, B. Ngwenya, K. M. Raletamo, and K. Andrae-Marobela, *Anal. Chim. Acta*, 2012, **730**, 42–48. <https://doi.org/10.1016/j.aca.2011.11.067>
60. A. Sadhu, P. Upadhyay, P. K. Singh, A. Agrawal, K. Ilango, D. Karmakar, G. P. I. Singh, and G. P. Dubey, *Environ. Monit. Assess.*, 2015, **187**, 542. <https://doi.org/10.1007/s10661-015-4764-3>
61. X.-H. Wu, D.-H. Sun, Z.-X. Zhuang, X.-R. Wang, H.-F. Gong, J.-X. Hong, and F. S. C. Lee, *Anal. Chim. Acta*, 2002, **453**, 311–323. [https://doi.org/10.1016/S0003-2670\(01\)01442-8](https://doi.org/10.1016/S0003-2670(01)01442-8)
62. X. Wu, Z. Zhong, K. Lin, X. Liu, Z. Wu, Z. Liu, and Y. Li, *Front. Pharmacol.*, 2022, **13**, 967608. <https://doi.org/10.3389/fphar.2022.967608>
63. H. Adugna, D. Ezez, A. Guadie, and M. Tefera, *J. Agr. Food Res.*, 2024, **16**, 101190. <https://doi.org/10.1016/j.jafr.2024.101190>
64. F. Karahan, I. I. Ozyigit, I. A. Saracoglu, I. E. Yalcin, A. H. Ozyigit, and A. Ilcim, *Biol. Trace Elem. Res.*, 2020, **197**, 316–329. <https://doi.org/10.1007/s12011-019-01974-2>
65. I. I. Ozyigit, F. Karahan, I. E. Yalcin, A. Hocaoglu-Ozyigit, and A. Ilcim, *Arab. J. Geosci.*, 2021, **15**, 27. <https://doi.org/10.1007/s12517-021-09264-9>
66. X. Bo-Yang, Z. Si-Qi, C. Xian-Xin, X. Yu, and L. Ji-Wu, *Curr. Pharm. Anal.*, 2022, **18**, 193–198. <http://dx.doi.org/10.2174/157341291766621021102281>
67. O. M. Oladeji, B. G. Kopaopa, L. L. Mungivha, and J. O. Olowoyo, *Biol. Trace Elem. Res.*, 2024, **202**, 178–186. <https://doi.org/10.1007/s12011-023-03701-4>
68. V. Kamar, R. Dağalp, and M. Taştekin, *Biol. Trace Elem. Res.*, 2018, **185**, 226–235. <https://doi.org/10.1007/s12011-017-1223-8>
69. P.-C. Zheng, X.-J. Li, J.-M. Wang, S. Zheng, and H.-D. Zhao, *Acta Phys. Sin.*, 2019, **68**, 125202. <https://doi.org/10.7498/aps.68.20190148>
70. D. Sun, F. Yang, M. Su, W. Han, and C. Dong, *Microw. Opt. Techn. Lett.*, 2023, **65**, 1200–1207. <https://doi.org/10.1002/mop.33240>
71. K. Nomita Devi and H. Nandakumar Sarma, *Nucl. Instrum. Meth. B*, 2010, **268**, 2144–2147. <https://doi.org/10.1016/j.nimb.2010.02.036>
72. F. Sánchez-Lara, E. Manzanera-Acuña, V. Badillo-Almaraz, R. Gutiérrez-Hernández, K. K. García-Aguirre, M. E. Vargas-Díaz, Á. O. Hernández-Rangel, K. M. Hernández-Sánchez, and M. C. Escobar-León, *Appl. Sci.* 2022, **12**, 11772. <https://doi.org/10.3390/app122211772>
73. E. V. Chuparina and T. S. Aisueva, *Environ. Chem. Lett.*, 2011, **9**, 19–23. <https://doi.org/10.1007/s10311-009-0240-z>
74. S. Kabir, M. A. Islam, and M. B. Hossen, *J. Radioanal. Nucl. Ch.*, 2023, **332**, 3687–3696. <https://doi.org/10.1007/s10967-023-09047-4>
75. E. Furuta, S. Ishihara, R. Okumura, and Y. Iinuma, *J. Radioanal. Nucl. Ch.*, 2015, **304**, 501–507. <https://doi.org/10.1007/s10967-014-3823-5>
76. Y.-Y. Yuan, Y.-T. Hao, D. Zeng, P. Pan, J.-X. Lu, B. Zhang, S.-N. He, A.-P. Xing, S.-Q. Chen, and J. Yuan, *Spectrochim. Acta A*, 2024, **317**, 124407. <https://doi.org/10.1016/j.saa.2024.124407>
77. J. H. He, Y. Y. Cheng, T. Yang, H. Y. Zou, and C. Z. Huang, *Anal. Chim. Acta*, 2018, **1035**, 203–210. <https://doi.org/10.1016/j.aca.2018.06.053>
78. A. Huang, X. Yang, T. Xia, D. He, R. Zhang, Z. Li, S. Yang, Y. Liu, and X. Wen, *Microchem. J.*, 2022, **179**, 107639. <https://doi.org/10.1016/j.microc.2022.107639>
79. Z. Li, X. Yang, Y. Zhou, A. Huang, Y. Sun, Z. Duan, S. Yang, C. Liao, Y. Liu, and X. Wen, *Microchem. J.*, 2023, **193**, 109135. <https://doi.org/10.1016/j.microc.2023.109135>
80. X. Zhao, X. Zhang, Q. Li, Y. Song, J. Zhang, Y. Yang, X. Xia, and Q. Han, *J. Food Meas. Charact.*, 2022, **16**, 2459–2467. <https://doi.org/10.1007/s11694-022-01356-8>
81. T. M. Galal, E. A. Farahat, M. M. El-Midany, and L. M. Hassan, *Rend. Lincei*, 2016, **27**, 241–250. <https://doi.org/10.1007/s12210-015-0468-4>
82. N. A. D'yakova, I. A. Samylina, A. I. Slivkin, S. P. Gaponov, and A. A. Myndra, *Pharm. Chem. J.*, 2018, **52**, 220–223. <https://doi.org/10.1007/s11094-018-1797-2>
83. D. Kostic, B. Arsic, S. Radelović, A. Pavlović, S. Tošić, and G. Stojanović, *Water Air Soil Poll.*, 2019, **230**, 98. <https://doi.org/10.1007/s11270-019-4153-6>
84. Y.-k. Liu, H.-W. Sun, C.-G. Yuan, and X.-P. Yan, *Anal. Chem.*, 2002, **74**, 1525–1529. <https://doi.org/10.1021/ac0156971>
85. K. Marschner, S. Musil, and J. Dědina, *Anal. Chem.*, 2016, **88**, 4041–4047. <https://doi.org/10.1021/acs.analchem.6b00370>
86. E. A. Lima, F. A. S. Cunha, M. J. Oliveira, W. S. Lyra, M. M. S. Junior, J. C. C. Santos, S. L. C. Ferreira, M. C. U. Araujo, and L. F. Almeida, *Food Chem.*, 2022, **381**, 132194. <https://doi.org/10.1016/j.foodchem.2022.132194>
87. S. O. Souza, D. V. L. Ávila, V. Cerdà, and R. G. O. Araujo, *Food Chem.*, 2022, **367**, 130673. <https://doi.org/10.1016/j.foodchem.2021.130673>
88. Erdiwansyah, A. Gani, H. Desvita, Mahidin, Bahagia, R. Mamat, and S. M. Rosdi, *Rineng*, 2025, **25**, 103717. <https://doi.org/10.1016/j.rineng.2024.103717>
89. J.-M. An, S. H. Hur, H. Kim, J. H. Lee, Y.-K. Kim, K. S. Sim, S.-E. Lee, and H. J. Kim, *Food Chem.*, 2024, **437**, 137836. <https://doi.org/10.1016/j.foodchem.2023.137836>
90. J. Naozuka, A. P. de Oliveira, H. B. de Oliveira, L. d. O. Lima, and C. S. Nomura, *ACS Omega*, 2025, **10**, 50695–50708. <https://doi.org/10.1021/acsoomega.5c05971>
91. Y. Zhou, L. Li, Z. Tang, Y. Zhang, Y. Xu, Z. Zheng, J. Yang, X. Hu, B. Wang, J. Zhang, Q. Jiang, and Y. Wang, *Food Chem.*, 2025, **481**, 144076. <https://doi.org/10.1016/j.foodchem.2025.144076>
92. V. Palleschi, S. Legnaioli, F. Poggialini, F. O. Bredice, I. A. Urbina, N. Lellouche, and S. Messaoud Aberkane, *Nat. Rev. Method Prime.*, 2025, **5**, 17. <https://doi.org/10.1038/s43586-025-00388-w>
93. S. Yao, Z. Yu, Z. Hou, L. Guo, L. Zhang, H. Ding, Y. Lu, Q. Wang, and Z. Wang, *TrAC, Trends Anal. Chem.*, 2024, **177**, 117795. <https://doi.org/10.1016/j.trac.2024.117795>
94. M. Markiewicz-Keszycyca, X. Cama-Moncunill, M. P. Casado-Gavaldà, Y. Dixit, R. Cama-Moncunill, P. J. Cullen, and C. Sullivan, *Trends Food Sci. Tech.*, 2017, **65**, 80–93. <https://doi.org/10.1016/j.tifs.2017.05.005>
95. M. Gu, H. Huang, Q. Jiao, D. Ma, Y. Xu, C. Liu, J. Li, X. Zhang, M. Yang, L. Xu, S. Jiang, H. Li, J. Qi, J. Zhang, and X. Tan, *J. Anal.*

- Atom. Spectrom.*, 2026, **41**, 416–425. <https://doi.org/10.1039/D5JA00355E>
96. B. Han, W. Gao, J. Feng, A. Iroshan, J. Yang, G. Chen, Y. Zhang, N. Aizezi, and Y. Liu, *J. Hazard. Mater.*, 2025, **496**, 139284. <https://doi.org/10.1016/j.jhazmat.2025.139284>
 97. K. M. Zierold, M. J. Smith, J. Xu, L. Cai, and L. Sears, *Cardiovasc. Toxicol.*, 2025, **25**, 969–978. <https://doi.org/10.1007/s12012-025-10011-9>
 98. P. Sukum, P. Narongchai, D. Boonyawan, S. Narongchai, and U. Tippawan, *Biol. Trace Elem. Res.*, 2019, **192**, 330–335. <https://doi.org/10.1007/s12011-019-01669-8>
 99. Y. Sunitha, A. Sarkar, and S. Kumar, *Anal. Method*, 2016, **8**, 7116–7123. <https://doi.org/10.1039/C6AY01855F>
 100. S. W. Raja, R. Acharya, A. D. Gandhi, and J. B. Singh, *J. Anal. Atom. Spectrom.*, 2024, **39**, 1919–1926. <https://doi.org/10.1039/D4JA00175C>
 101. K. N. Devi, H. N. Sarma, and S. Kumar, *Nucl. Instrum. BETH B*, 2008, **266**, 1605–1610. <https://doi.org/10.1016/j.nimb.2007.12.004>
 102. K. Sanyal and S. Dhara, *TrAC, Trends Anal. Chem.*, 2025, **193**, 118464. <https://doi.org/10.1016/j.trac.2025.118464>
 103. R. Ferraz de Camargo, T. Rodrigues Tavares, F. Rodrigues dos Santos, and H. W. Pereira de Carvalho, *Food Chem.*, 2025, **473**, 143095. <https://doi.org/10.1016/j.foodchem.2025.143095>
 104. D. A. Ahumada-Forigua, E. Fernández, A. Rossell, N. Verger, J. Saurina, and J. F. García, *Anal. Chim. Acta*, 2026, **1386**, 345038. <https://doi.org/10.1016/j.aca.2025.345038>
 105. A. J. Specht, J. F. Obrycki, M. Mazumdar, and M. G. Weisskopf, *Environ. Sci. Technol.*, 2021, **55**, 5050–5055. <https://doi.org/10.1021/acs.est.0c06622>
 106. J. L. Lavers, N. R. Howell, A. L. Bond, D. L. Howard, M. D. de Jonge, L. Puskar, and R. B. Banati, *J. Hazard. Mater.*, 2025, **494**, 138528. <https://doi.org/10.1016/j.jhazmat.2025.138528>
 107. I. J. Kim, R. P. Watson, and R. M. Lindstrom, *Anal. Chem.*, 2011, **83**, 3493–3498. <https://doi.org/10.1021/ac200158e>
 108. C. M. Salgado, R. Sophia de Freitas Dam, W. L. Salgado, C. de Carvalho Conti, and J. C. Suita, *Radiat. Phys. Chem.*, 2025, **232**, 112699. <https://doi.org/10.1016/j.radphyschem.2025.112699>
 109. D. D. Das, N. Sharma, and P. A. Chawla, *Crit. Rev. Anal. Chem.*, 2024, **54**, 2450–2466. <https://doi.org/10.1080/10408347.2023.2178841>
 110. J. Cai, J. Bai, C.-B. Ma, X. Bai, and M. Zhou, *TrAC, Trends Anal. Chem.*, 2026, **194**, 118551. <https://doi.org/10.1016/j.trac.2025.118551>
 111. I. D. Charles, Z. Xu, T. Qin, Z. Xun, S. Zhang, L. Wang, and B. Liu, *TrAC, Trends Anal. Chem.*, 2026, **194**, 118540. <https://doi.org/10.1016/j.trac.2025.118540>
 112. N. Ullah, M. Mansha, I. Khan, and A. Qurashi, *TrAC, Trends Anal. Chem.*, 2018, **100**, 155–166. <https://doi.org/10.1016/j.trac.2018.01.002>
 113. J. X. Xu, Y. Yuan, S. Zou, O. Chen, and D. Zhang, *Anal. Chem.*, 2019, **91**, 8540–8548. <https://doi.org/10.1021/acs.analchem.9b01803>
 114. G. Lin, Z. Zhao, Z. Liu, Y. Li, R. Zhou, and Y. Fu, *Anal. Chem.*, 2025, **97**, 19437–19444. <https://doi.org/10.1021/acs.analchem.5c01285>
 115. W. Yang, L. Ye, Y. Wu, X. Wang, S. Ye, Y. Deng, K. Huang, H. Luo, J. Zhang, and C. Zheng, *J. Hazard. Mater.*, 2024, **470**, 134038. <https://doi.org/10.1016/j.jhazmat.2024.134038>
 116. S. Ye, B. Yu, T. Ren, Y. Lin, J. Zhang, and C. Zheng, *Anal. Chem.*, 2023, **95**, 13949–13956. <https://doi.org/10.1021/acs.analchem.3c02531>
 117. K. Mandal and N. K. Dhal, *Environ. Sci. Pollut. R.*, 2023, **30**, 43860–43871. <https://doi.org/10.1007/s11356-023-25396-9>
 118. A. Petukhov, T. Kremleva, G. Petukhova, and N. Khritokhin, *Toxicol.* 2021, vol. 9.
 119. R. Zhang, C. Yan, X. Yang, K. Hu, F. Hao, S. Yang, Q. Deng, Z. Duan, Y. Liu, and X. Wen, *Anal. Chim. Acta*, 2023, **1251**, 340992. <https://doi.org/10.1016/j.aca.2023.340992>
 120. R. Zhang, X. Yang, Y. Liu, J. Hu, K. Hu, Y. Liu, Q. Deng, S. Yang, F. Hao, and X. Wen, *Talanta*, 2024, **271**, 125721. <https://doi.org/10.1016/j.talanta.2024.125721>
 121. H. Chi, X. Liu, T. Xia, X. Yang, D. He, Z. Li, Y. Liu, N. Lu, S. Yang, Z. Li, and X. Wen, *Microchem. J.*, 2023, **194**, 109342. <https://doi.org/10.1016/j.microc.2023.109342>
 122. B. Fattahi, K. Arzani, M. K. Souiri, and M. Barzegar, *Ind. Crop. Prod.*, 2021, **171**, 113979. <https://doi.org/10.1016/j.indcrop.2021.113979>
 123. S. Terfi, D. Zineb, K. Soumeiya, and F. and Sadi, *Drug Chem. Toxicol.*, 2023, **46**, 864–878. <https://doi.org/10.1080/01480545.2022.2104868>
 124. J. Wang and Y. Liu, *Env. Pollut. Bioavail.*, 2023, **35**, 2223768. <https://doi.org/10.1080/089026395940.2023.2223768>
 125. X. Qian, Y. Luo, H. Yang, J. Wang, H. Zhang, H. Shi, Q. Li, Z. Song, B. Hao, and W. Fan, *Front. Env. Sci.*, 2025, **13**, 1602385. <https://doi.org/10.3389/fenvs.2025.1602385>
 126. Y. Gong, W. Ren, F. Li, Y. Jiang, and Z. Zhang, *Environ. Technol. Innov.*, 2025, **36**, 103800. <https://doi.org/10.1016/j.eti.2024.103800>
 127. H. X. Yang, H. Chi, X. Liu, N. Lu, Y. Liu, S. Yang, and X. Wen, *Microchem. J.*, 2024, **207**, 111958. <https://doi.org/10.1016/j.microc.2024.111958>
 128. L. Yang, Y. Kang, N. Li, Y. Wang, H. Sun, T. Ao, L. Chen, and W. Chen, *Sci. Total Environ.*, 2024, **913**, 169741. <https://doi.org/10.1016/j.scitotenv.2023.169741>
 129. M. Liu, X. Du, M. Wang, Y. Huo, Y. Zeng, J. Wu, X. Ying, F. Wei, L. Liu, and J. Tang, *Ecotox. Environ. Safe.*, 2025, **291**, 117839. <https://doi.org/10.1016/j.ecoenv.2025.117839>
 130. S.-q. Niu, T. Li, X.-w. Bao, X.-l. Qian, F.-l. Yang, S. Wu, S.-y. Li, L.-l. Liang, J. Bai, S.-j. Liu, Y. Li, and J.-l. Guo, *Plant Physiol. Bioch.*, 2026, **232**, 111089. <https://doi.org/10.1016/j.plaphy.2026.111089>
 131. S.-q. Niu, T. Li, X.-w. Bao, J. Bai, L. Liu, S.-j. Liu, W. Qin, Y. Li, and J.-l. Guo, *Stress Bio.*, 2024, **4**, 44. <https://doi.org/10.1007/s44154-024-00187-5>
 132. Y. Wang, X. Zhou, F. Kong, Z. Qi, and M. Yu, *Ind. Crop. Prod.*, 2025, **223**, 120295. <https://doi.org/10.1016/j.indcrop.2024.120295>
 133. I. D. de Souza, E. S. P. Melo, V. A. Nascimento, H. S. Pereira, K. R. N. Silva, P. R. Espindola, P. F. S. Tschinkel, E. M. Ramos, F. J. M. Reis, I. B. Ramos, F. G. Paula, K. R. W. Oliveira, C. D. Lima, Â. A. Nunes, and V. A. do Nascimento, *BioMed Res. Int.*, 2021, **2021**, 6678931. <https://doi.org/10.1155/2021/6678931>
 134. D. J. Lawi, W. S. Abdulwhaab, and A. A. Abojassim, *Biol. Trace Elem. Res.*, 2023, **201**, 3528–3540. <https://doi.org/10.1007/s12011-022-03408-y>
 135. C. Meng, P. Wang, Z. Hao, Z. Gao, Q. Li, H. Gao, Y. Liu, Q. Li, Q. Wang, and F. Feng, *Environ. Geochem. Hlth.*, 2022, **44**, 817–828. <https://doi.org/10.1007/s10653-021-00978-z>
 136. F. Amerley Amarih, E. Selom Agorku, R. Bright Voegborlo, G. Winfred Ashong, E. Nii Klu Nortey, and N. Jackson Mensah, *J. Chem.*, 2023, **2023**, 9928577. <https://doi.org/10.1155/2023/9928577>
 137. F. Karahan, *Biol. Trace Elem. Res.*, 2023, **201**, 493–513. <https://doi.org/10.1007/s12011-022-03299-z>

138. Y. Huang, T. Ying, Z. Ning, F. Zhaocong, and W. and Ren, *Hum. Ecol. Risk Assess.*, 2018, **24**, 1312–1326.
<https://doi.org/10.1080/10807039.2017.1411782>

139. L. Zhou, S. Wang, Q. Hao, L. Kang, C. Kang, J. Yang, W. Yang, J. Jiang, L.-Q. Huang, and L. Guo, *Chin. Med-UK*, 2018, **13**, 40.
<https://doi.org/10.1186/s13020-018-0196-7>

140. T. Zuo, F. Luo, Y. Suo, Y. Chang, Z. Wang, H. Jin, J. Yu, S. Xing, Y. Guo, D. Wang, F. Wei, G. Wang, L. Sun, and S. Ma, *Toxics*, 2024, **12**, 528. <https://doi.org/10.3390/toxics12070528>

Pre-proof